Precision measurements of electroweak observables with the ATLAS detector

Camilla Vittori

Università di Bologna and INFN

On behalf of the ATLAS Collaboration

QCD@LHC 2017
Debrecen, August 28th-September 1st

Electroweak observables in W and Z processes

- High production rate with clean leptonic final states
- **Predictions** at NNLO QCD and NLO EW, **in many cases less precise than measurements**
  → Constraints on theory calculations (PDFs, scales) and associated uncertainties
- **Precision measurement of EW parameters like** $\boldsymbol{\sigma^{prod}}$, $\boldsymbol{A_{FB}}$, P_τ **and** $\boldsymbol{M_W}$

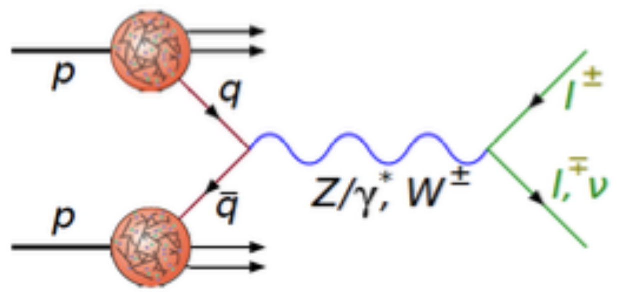

TALK FOCUSED ON

- **3D Z cross section @ 8 TeV**
  https://atlas.web.cern.ch/Atlas/GROUPS/PHYSICS/PAPERS/STDM-2016-04/
- **Tau Polarisation @ 8 TeV**
  ATLAS-CONF-2017-049
- **W/Z cross sections @ 13 TeV**
  Phys. Lett. B 759 (2016) 601
- **W mass @ 7 TeV**
  sub. to EPJC - arXiv:1701.07240

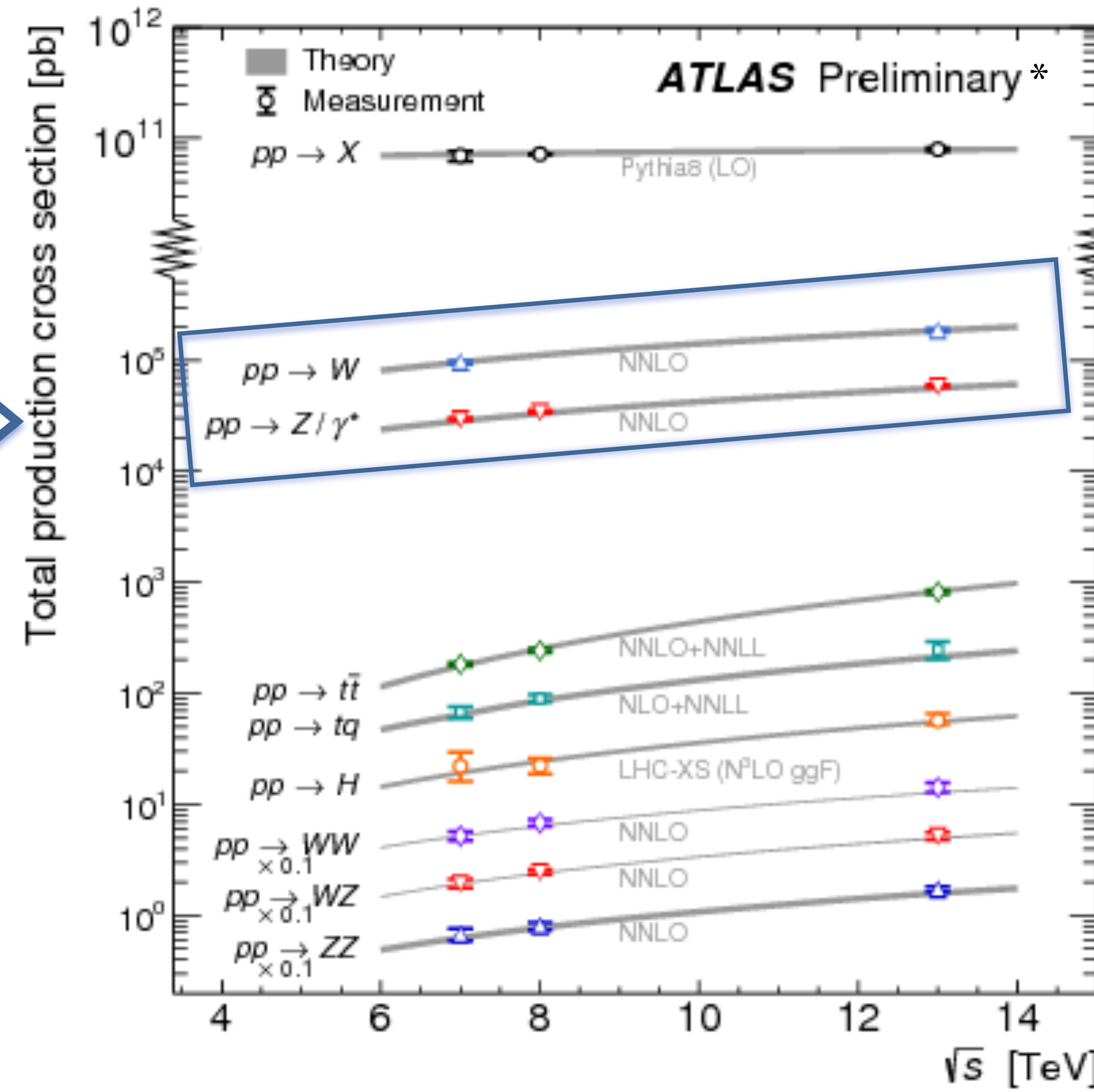

*https://atlas.web.cern.ch/Atlas/GROUPS/PHYSICS/CombinedSummaryPlots/SM/

3D Cross Section · **Motivations**

8 TeV, 20.2 fb^{-1}

- 3D cross section of Z Drell-Yan production as a function of **m_{ll}**, **$|y_{ll}|$** and **$\cos\vartheta^*$** in Collins-Soper frame
  - 1D and 2D cross sections as a function of m_{ll} and $|y_{ll}|$
  - Forward-backward asymmetry A_{FB} due to parity violation in Z production
    → A_{FB} referred to the **angular distributions of the outgoing leptons** with respect to incoming quark direction **in the dilepton rest frame**

Propagator with terms due to γ*, Z/γ* and Z exchange with different contribution at different m_{ll}

$$\frac{d^3\sigma}{dm_{ll}dy_{ll}dcos\theta^*} = \frac{\pi\alpha^2}{3m_{ll}s}\sum_q P_q[f_q(x_1,Q^2)f_{\bar{q}}(x_2,Q^2) + (q \leftrightarrow \bar{q})]$$

PDFs

- Z/γ* interference term generates the A_{FB} in $\cos\vartheta^*$
  → change sign at m_Z
  → increase with y_{ll} due to larger difference in sea and valence quarks

$$A_{FB} = \frac{d^3\sigma(cos\theta^* > 0) - d^3\sigma(cos\theta^* < 0)}{d^3\sigma(cos\theta^* > 0) + d^3\sigma(cos\theta^* < 0)}$$

- A_{FB} related to the weak mixing angle $\sin^2\vartheta_W$
  → LO EW: $\sin^2\vartheta_W = 1 - m_W^2/m_Z^2$

intrinsically linked to the W mass!

  - Measurements designed to be simultaneously sensitive to **$\sin^2\vartheta^{eff}$** and to **PDFs**
    → reduce the PDF-induced uncertainty on $\sin^2\vartheta^{eff}$

3D Cross Section · **Motivations**

8 TeV, 20.2 fb^{-1}

$$A_{FB} = \frac{d^3\sigma(cos\theta^* > 0) - d^3\sigma(cos\theta^* < 0)}{d^3\sigma(cos\theta^* > 0) + d^3\sigma(cos\theta^* < 0)}$$

Collins-Soper Frame

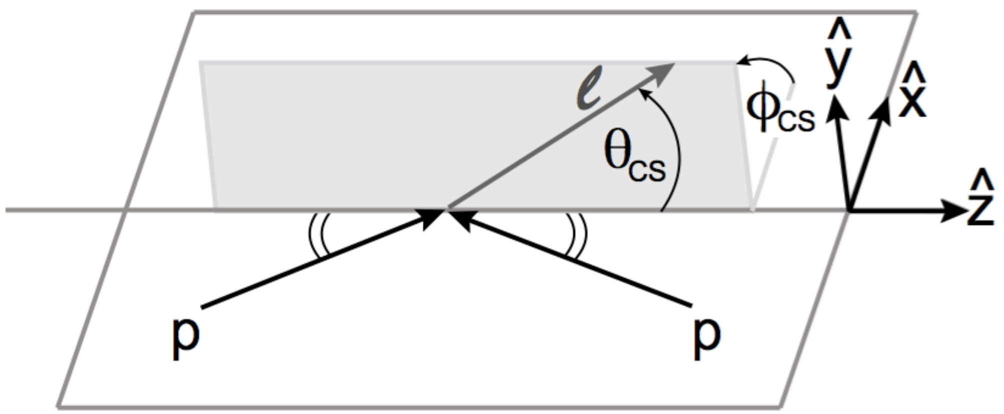

- Rest frame of di-lepton system
- cosϑ^* measured from the z-axis, symmetric to the 2 incoming partons.

$$cos\theta^* = \frac{p_{Z,ll}}{m_{ll}|p_{Z,ll}|}\frac{p_1^+p_2^- - p_1^-p_2^+}{\sqrt{m_{ll}^2 + p_{T,ll}^2}}$$

✤ Large PDF uncertainties in ATLAS measurement @ 7 TeV

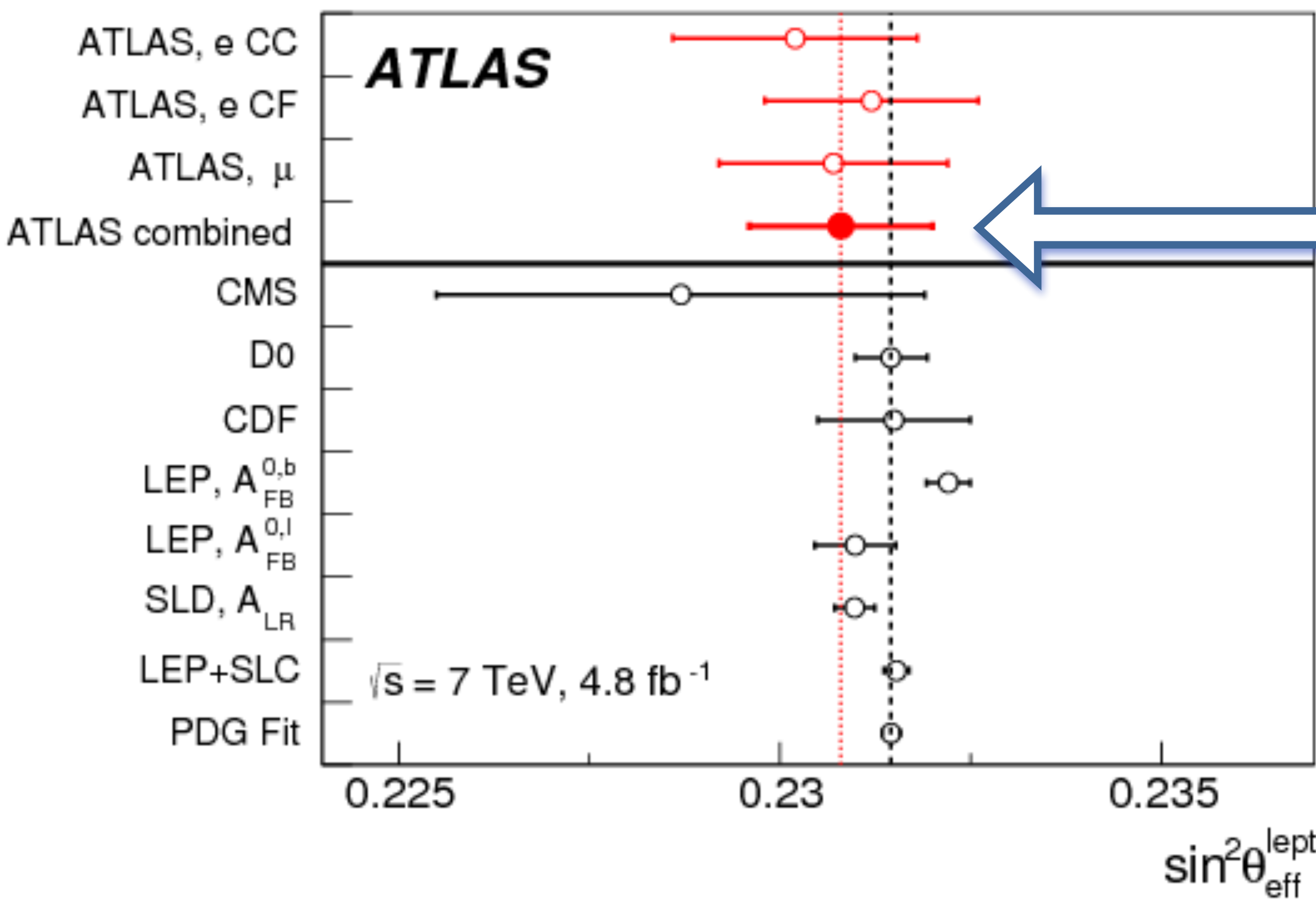

Uncertainty*	Lepton combined [10^{-4}]
PDFs	9
MC statistics	2
Electron energy scale	3
Electron energy resolution	2
Muon energy scale	2
High-order corrections	2
others	2

**JHEP 09 (2015) 049*

3D Cross Section · Selection

8 TeV, 20.2 fb^{-1}

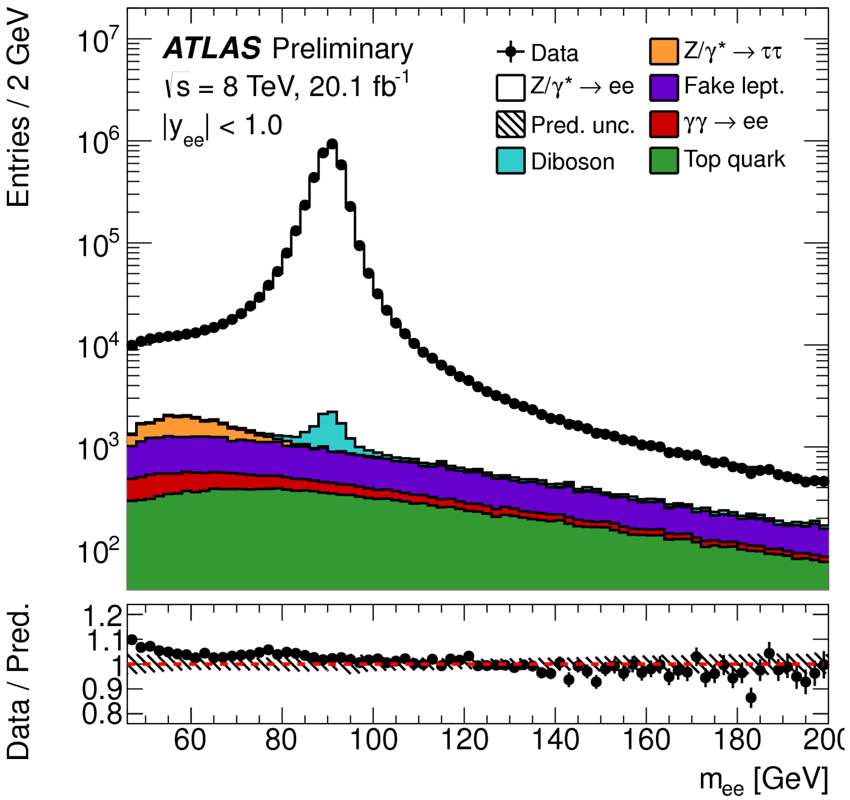

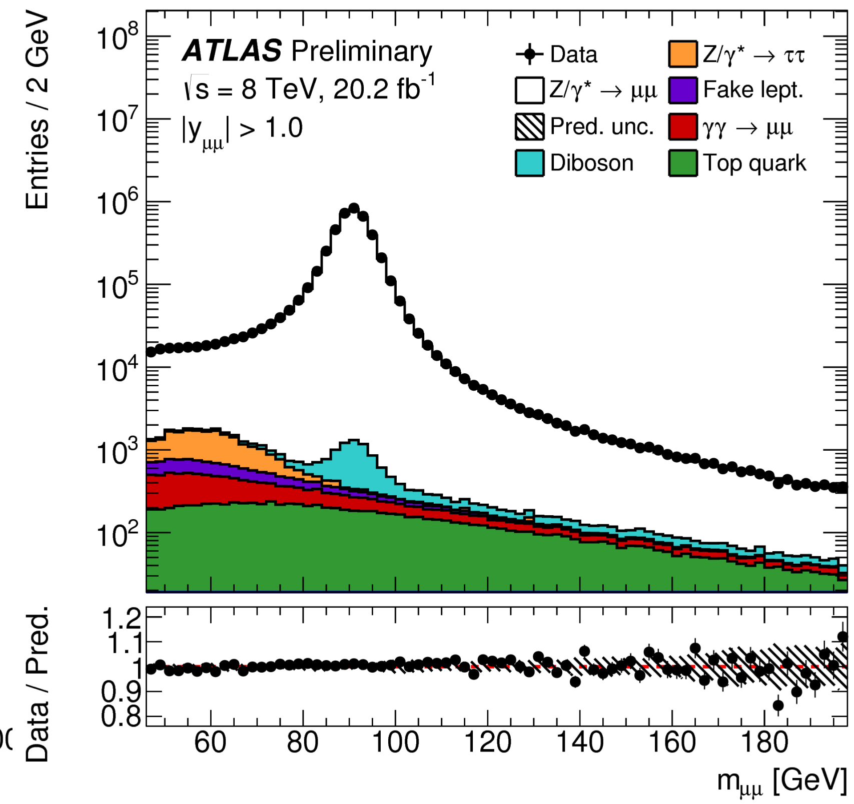

Central Selection

electrons and muons with **|η^l|<2.4** and **p$_T$^{l}>20 GeV**:

7 bins in $46<m_{ll}<200$ GeV
\+ 12 bins in $|y_{ll}|<2.4$
\+ 6 bins in $\cos\vartheta^*$
= **504 bins**

Forward Selection

1 central (p$_T$^{l}>25 GeV) and **1 forward (|η^l|>2.5 and p$_T$^{l}>20 GeV) electron**:

5 bins in $66<m_{ll}<150$
\+ 5 bins in $1.2|y_{ll}|<3.6$
\+ 6 bins in $\cos\vartheta^*$
= **150 bins**

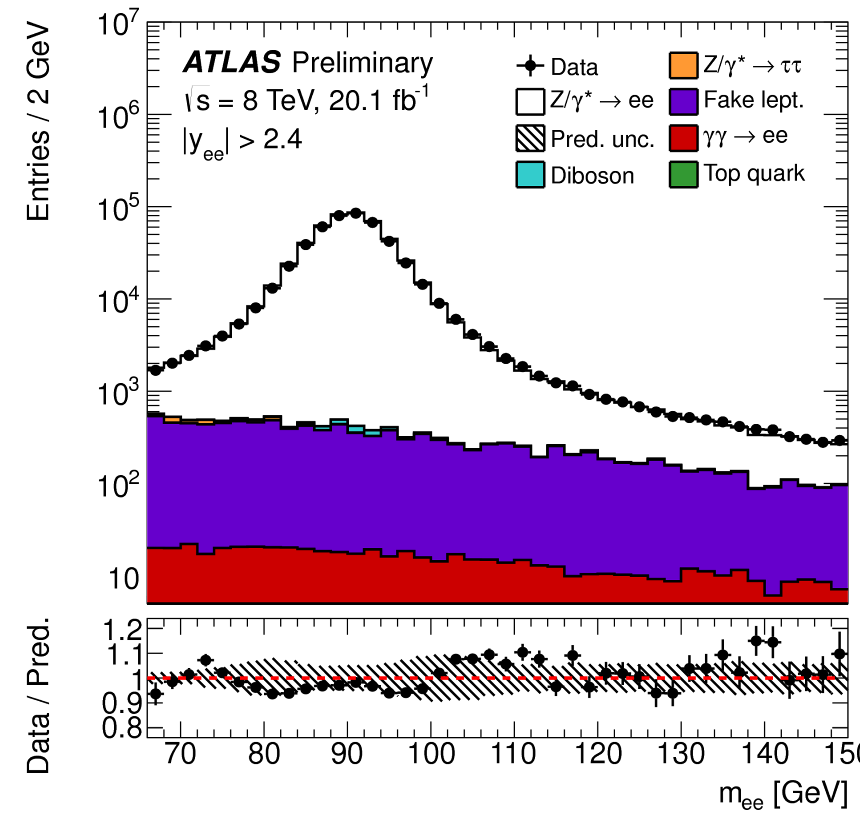

Z Drell-Yan signal from MC (Powheg+Pythia8) with mass-dependent NNLO/NLO k-factor and p_T^{ll}-dependent polarisation from DYNNLO.

3D Cross Section · cosϑ* at the Z peak   8 TeV, 20.2 fb^{-1}

- Bins **under Z peak:** 80<m_{ll}<91 GeV and 91<m_{ll}<102 GeV **symmetric** in cosϑ* and almost **background free** in central and forward regions.
- Analysis in the forward region allows to extend results in $|y_{ll}|$ and cosϑ*
- Main uncertainties due to reco+trigger+id efficiencies (<0.5%), JES and JER (~1%) and charge-dependent momentum reconstruction for muons (~1%)

Central Selection

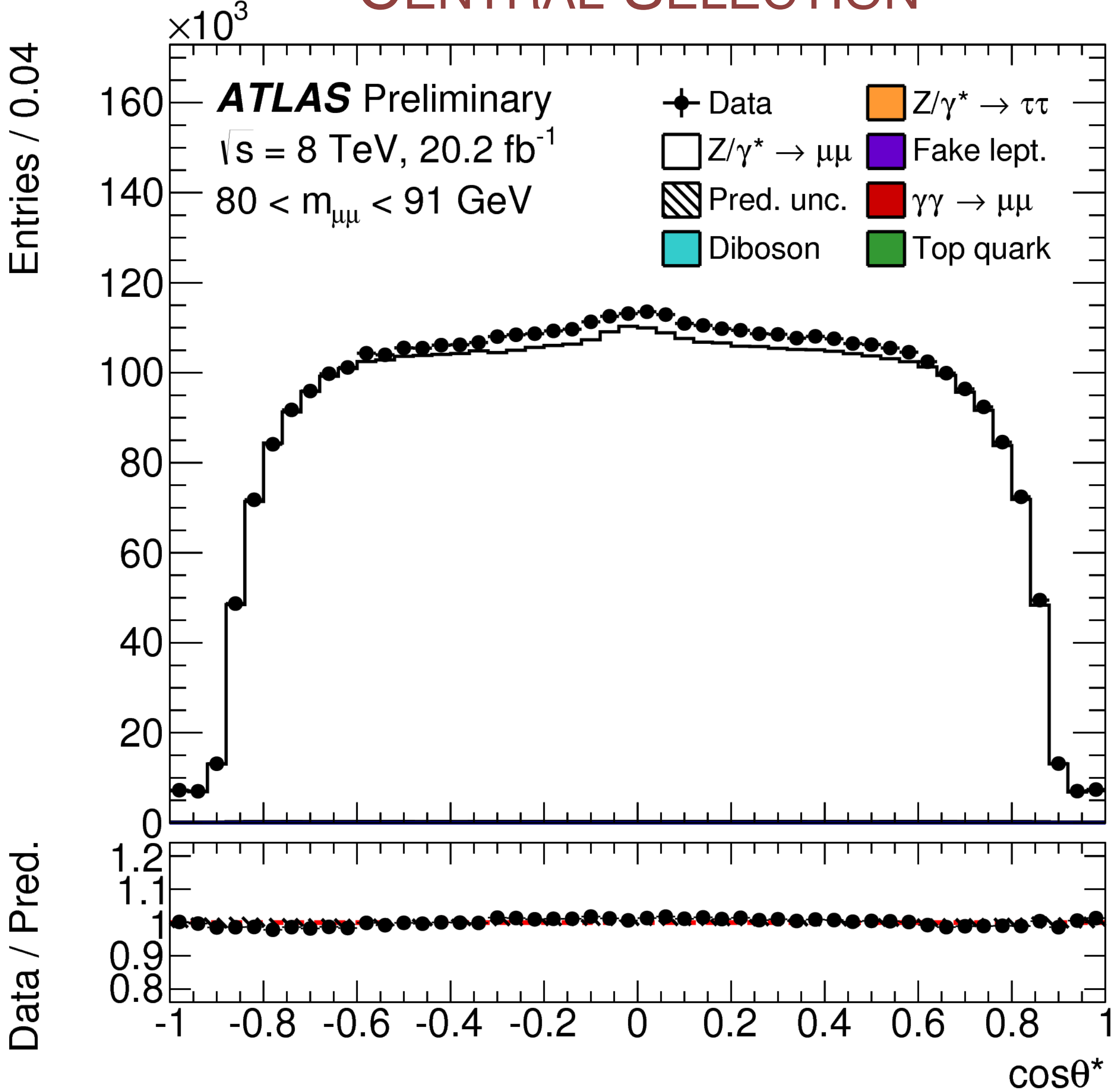

Forward Selection

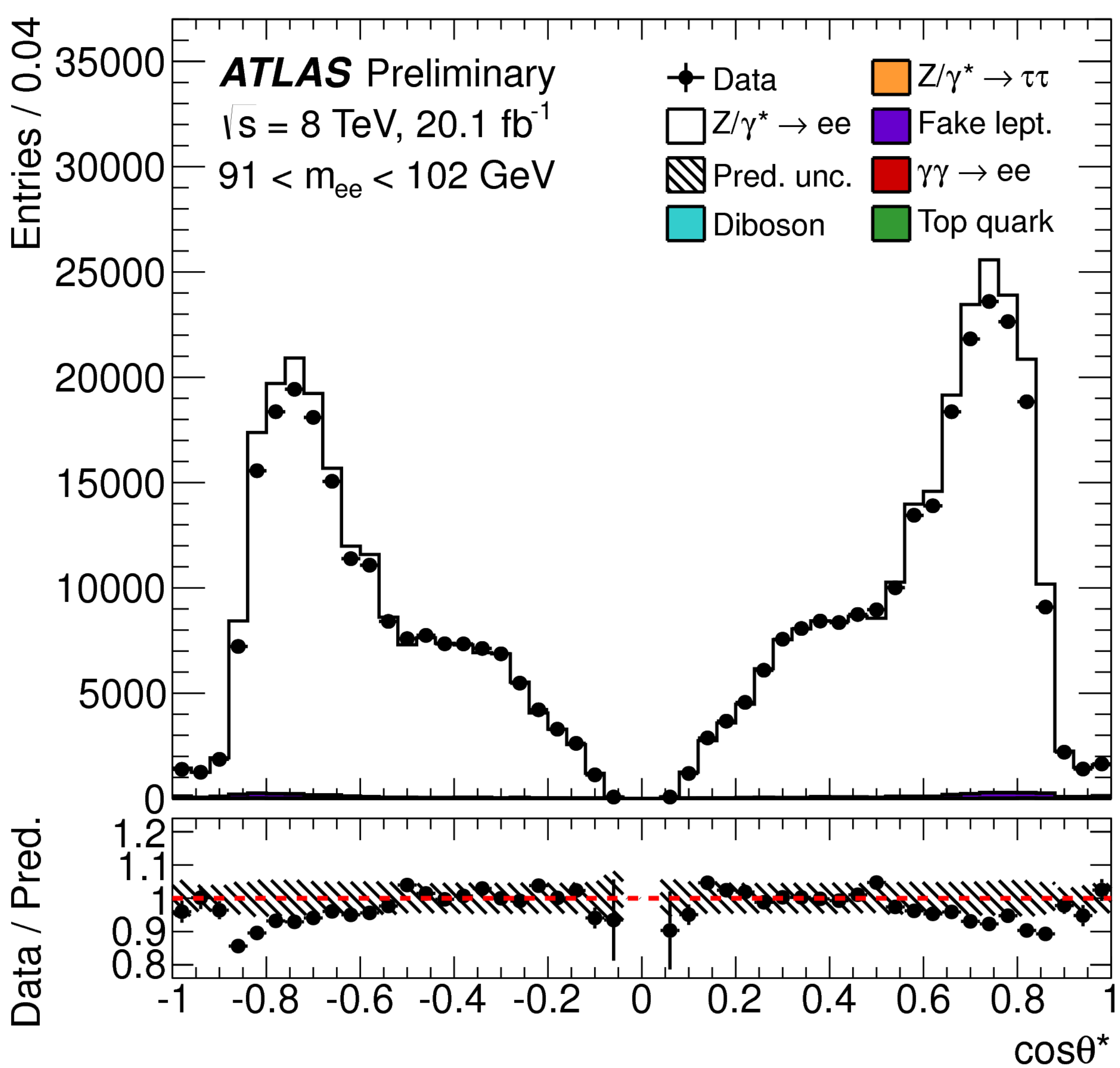

- Cross sections **first unfolded to dress level** (leptons after FSR recombined with the radiated photons), **then corrected to** born level using Powheg.
- Combined born-level measurements (central region) **integrated over the kinematic variables** → **$|y_{ll}|$ and $\cos\vartheta^*$ to determine $d\sigma/dm_{ll}$**
  → **$\cos\vartheta^*$ to determine $d^2\sigma/dm_{ll}dy_{ll}$**
- Cross sections first combined and then integrated (for $d\sigma/dm_{ll}$ $\chi^2/N_{DF} = 12.8/7$)

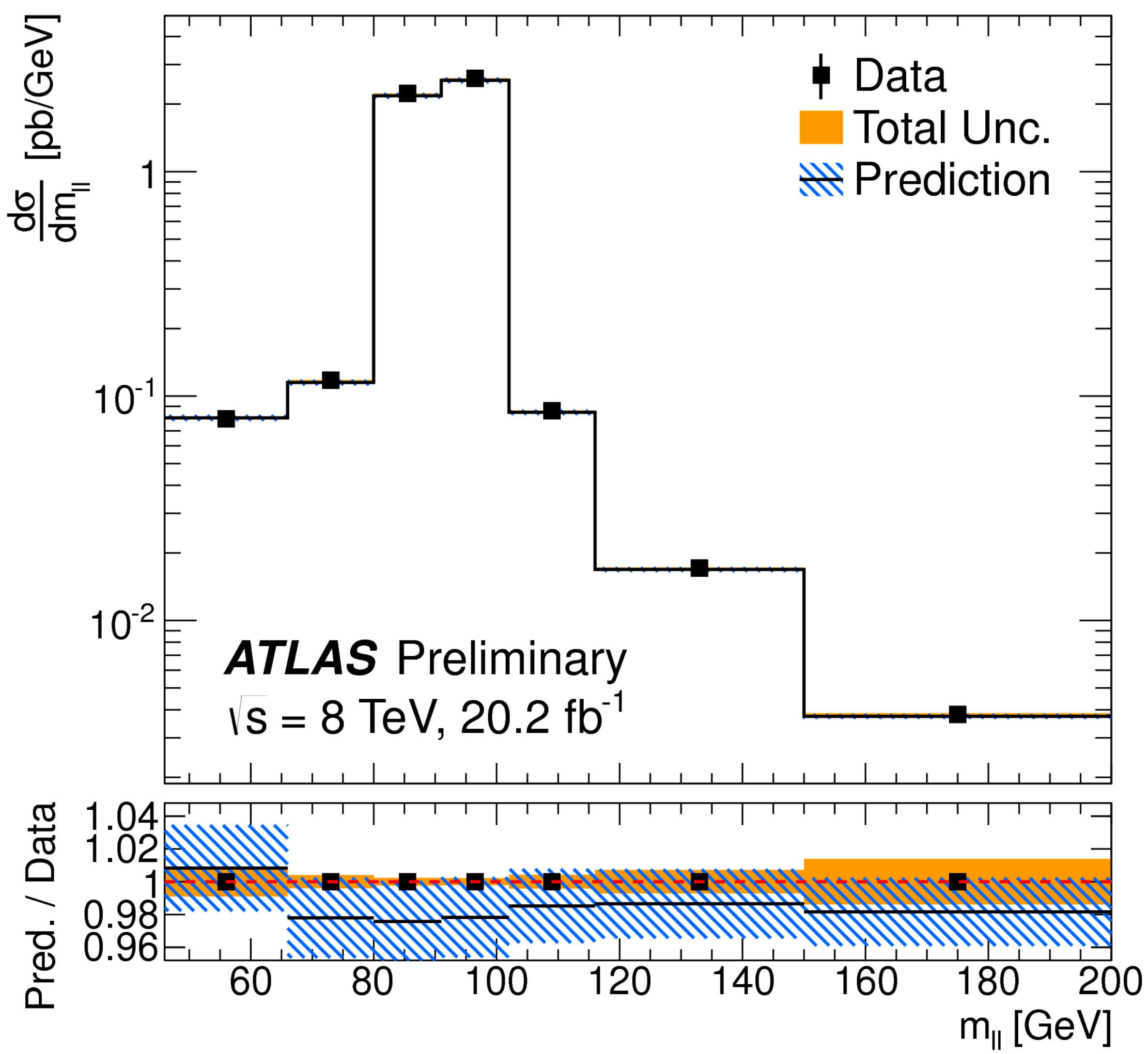

Data precision ~2%
(1.9% lumi + 0.5% syst. + 0.5% stat.)

Fiducial measurements well predicted by NLO Powheg+Pythia
→ the uncertainties in the predictions include PDFs and samples size

Predictions underestimate the cross sections by about ~1-2% (except in the low mass bin), within theoretical (PDF) uncertainties
↓
Data have a constraining power!

Double differential $d^2\sigma/dm_{ll}dy_{ll}$ cross section 8 TeV, 20.2 fb^{-1}

- Theoretical predictions are in good agreement with data, although with a tendency of underestimate data
- Good agreement between lepton channels with χ^2/N_{DF} = 103.4/84

Central bins around the Z peak

cross section precision ~0.4% (+1.9% lumi) **for $|y_{ll}|<1$** and **~0.7%** (+1.9% lumi) **at $|y_{ll}|=2.4$**

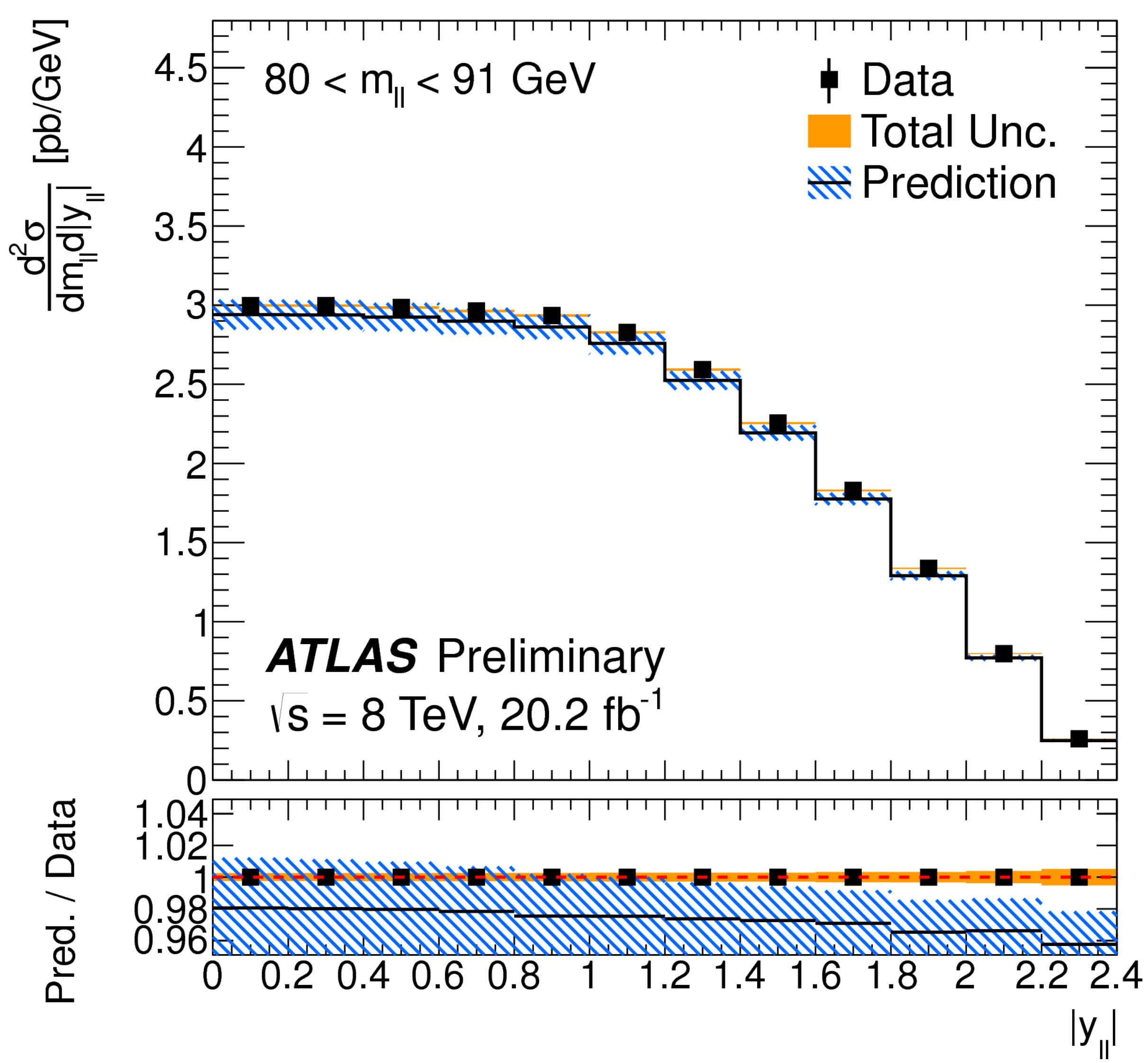

High mass bins

experimental and statistical uncertainties contribute equally, from **0.5% to 1.8%** (+1.9% lumi)

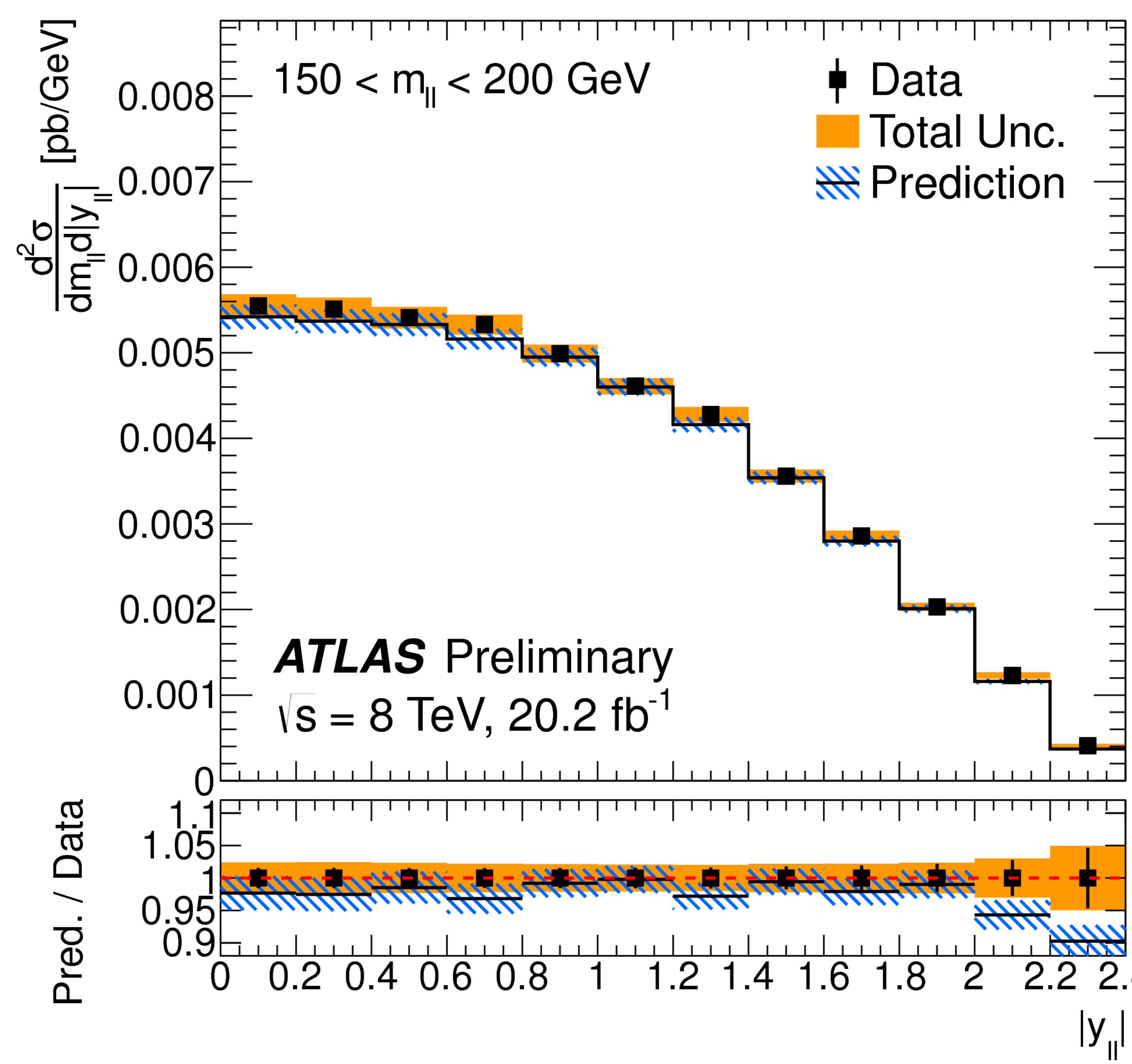

3D Cross Section

8 TeV, 20.2 fb^{-1}

- $A_{FB}<0$ below the Z peak, vanishing at $m_{ll} \sim m_Z$ and $A_{FB}>0$ above the Z peak
- cross section for large $\cos\vartheta^*$ increases with mass → reduced impact of fiducial cuts
- data precision <0.5% in the Z-peak region for $|y_{ll}|<1.4$

46-66 GeV | 80-91 GeV | 150-200 GeV

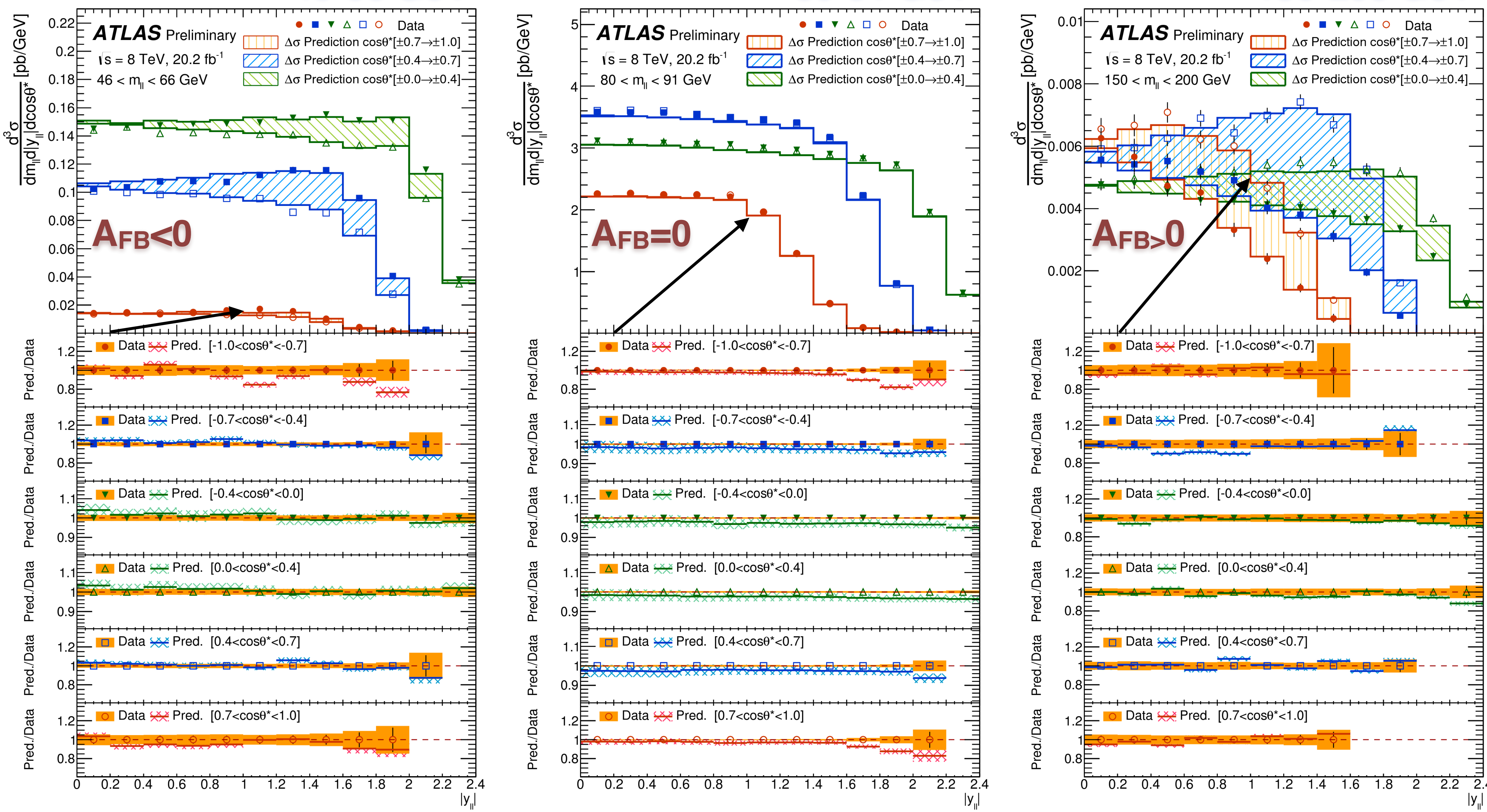

- Uncertainties symmetric in cosϑ^*, such as scale and resolution, cancel

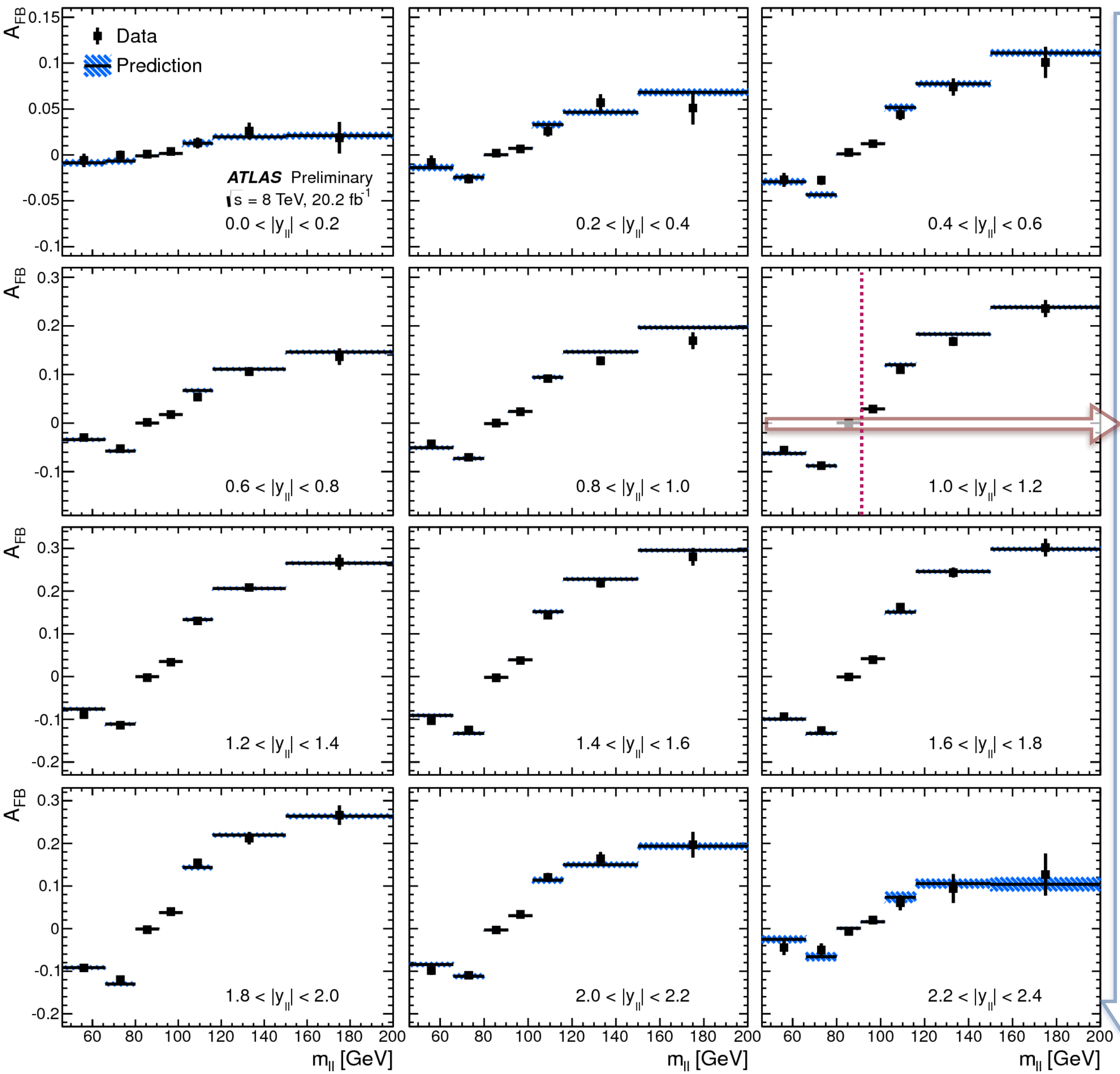

$$A_{FB} = \frac{d^3\sigma(cos\theta^* > 0) - d^3\sigma(cos\theta^* < 0)}{d^3\sigma(cos\theta^* > 0) + d^3\sigma(cos\theta^* < 0)}$$

A_{FB} increases with m_{ll}, flipping sign at $m_{ll}=m_Z$

At high $|y_{ll}|$ (larger x) valence quarks carry a larger momentum with a longitudinal boost → direction of incoming quarks well modelled by Powheg

Tau Polarisation (P_τ) 8 TeV, 20.2 fb^{-1}

- $Z \to \tau\tau$ events using τ leptonic decays as trigger and τ hadronic decays to study P_τ
- P_τ is a measure of the parity violation in $Z \to \tau\tau$ processes:

$$P_\tau = \frac{\sigma_+ - \sigma_-}{\sigma_+ + \sigma_-} \xrightarrow{\text{relativistic limit}} \frac{\sigma_{RH} - \sigma_{LH}}{\sigma_{RH} + \sigma_{LH}}$$

Asymmetry of the cross section for +/- helicity states

- Pioneer for experimental techniques in $H \to \tau\tau$ and searches
- Tau helicity affects the decay kinematics
  → Sensitive variable Υ
  h^0: neutral decay particles

$$\Upsilon = \frac{E_T^{\pi^\pm} - E_T^{h^0}}{E_T^{\tau^\pm}} = 2\frac{p_T^{\pi^\pm}}{E_T^{\tau^\pm}} - 1$$

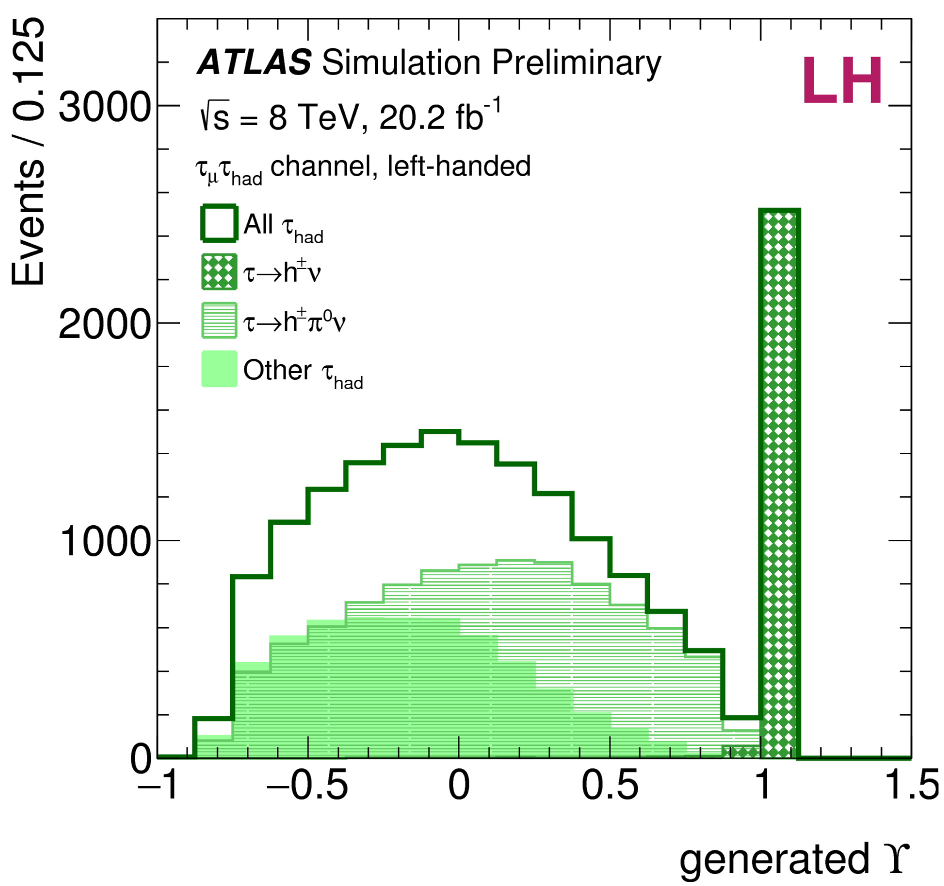

- largest contribution from $\tau^\pm \to \pi^\pm\pi^0\nu$
- difference in LH and RH Υ shapes for $\tau^\pm \to \pi^\pm N\pi^0\nu$ with $N \geq 1$
- $\tau^\pm \to \pi^\pm\nu$ sensitivity from acceptance and efficiencies

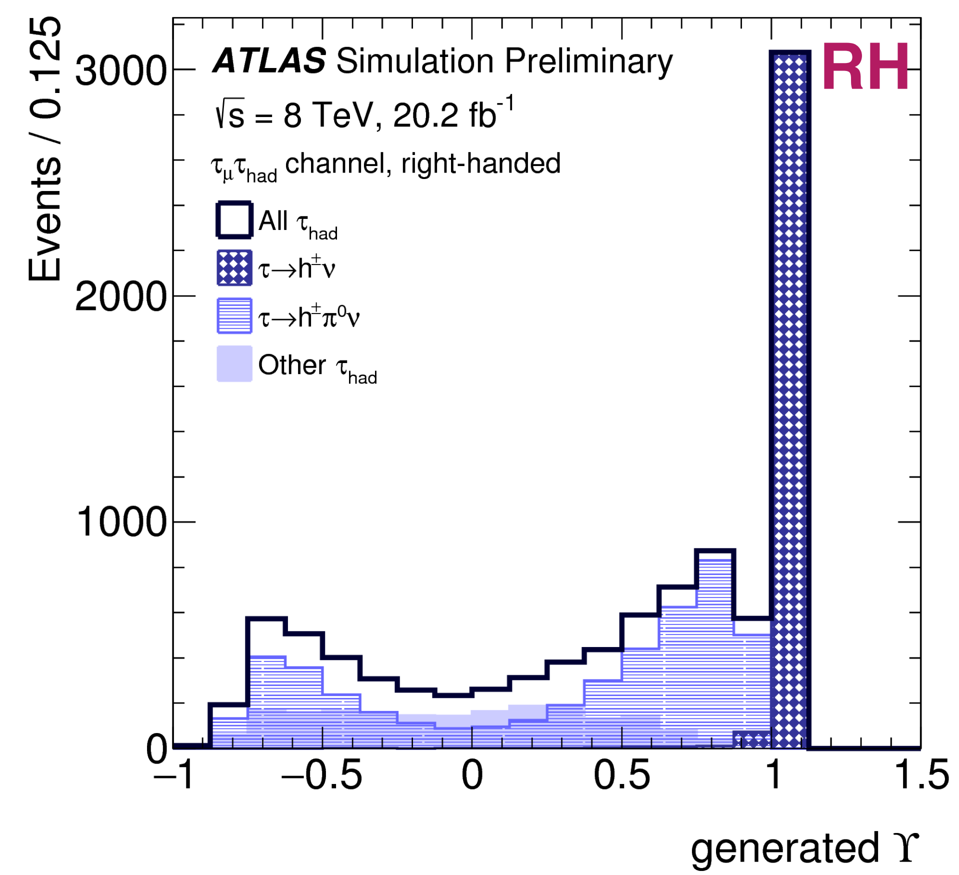

- **P_τ from fit on Υ distribution** for electron, muon channels and combination

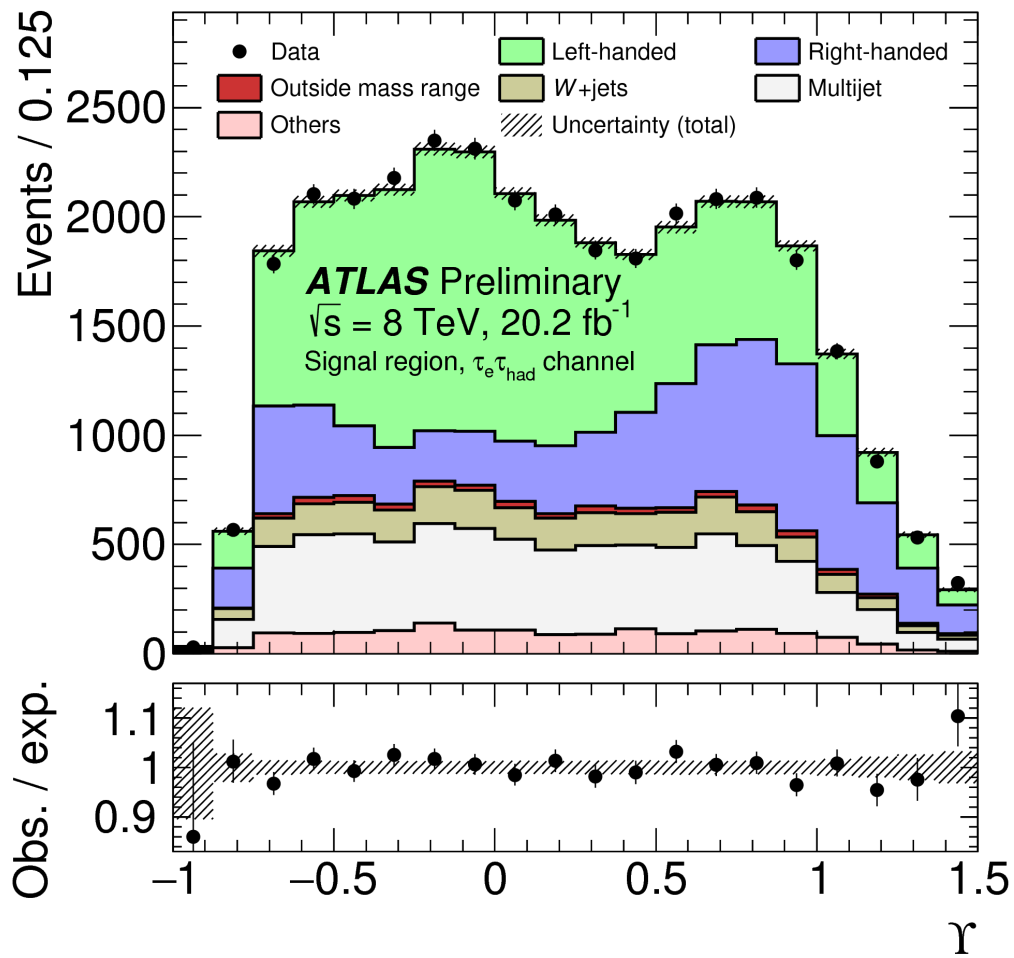

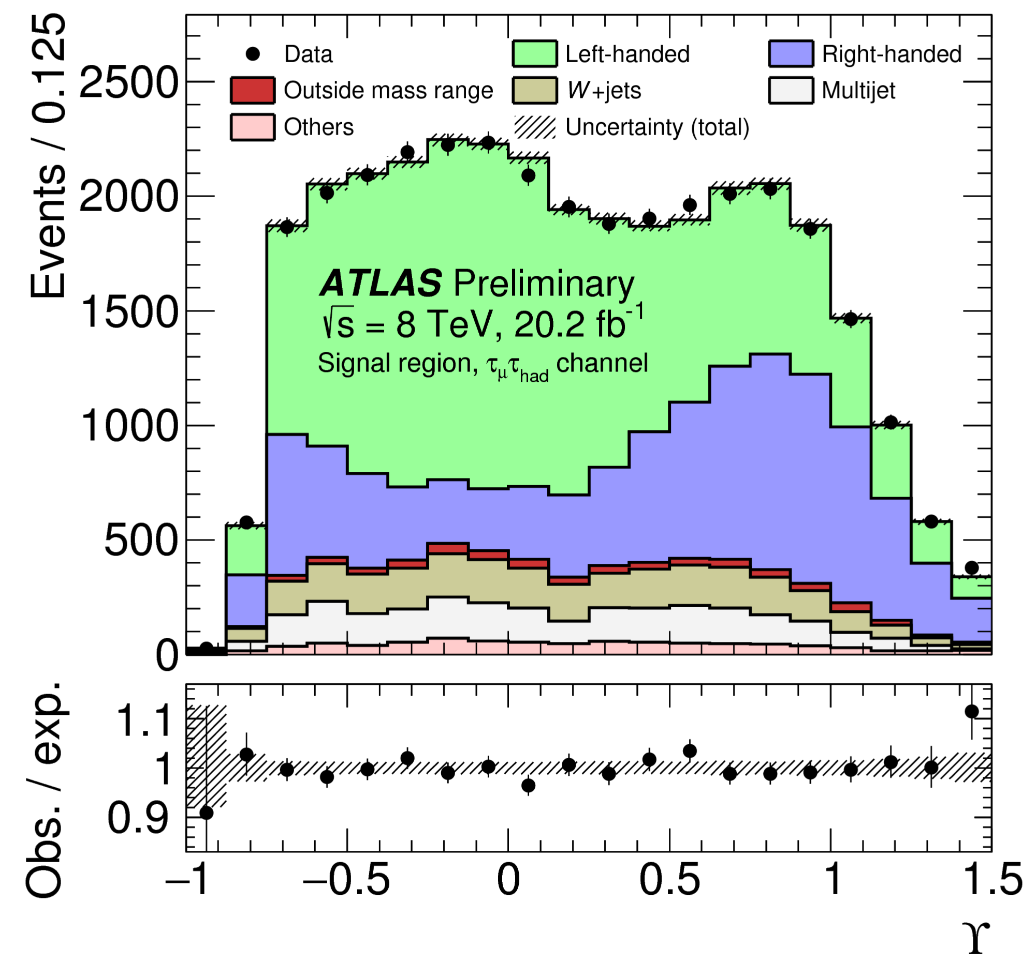

- Fiducial results are extrapolated to $66<m_{Z/\gamma^*}<116$ mass.

	Measured P_τ	SM predicted P_τ
Fiducial region	-0.27 ± 0.02 (stat.) ± 0.04 (syst.)	-0.270 ± 0.06
Mass range $66<m_{Z/\gamma^*}<116$	-0.14 ± 0.02 (stat.) ± 0.04 (syst.)	-0.1517 ± 0.019

◁Results in agreement with expectations based on ALPGEN+PYTHIA6 +Tauola

W and Z cross sections

13 TeV, 81 pb^{-1}

- Precise test of lepton universality ← Ratio of cross sections in different lepton final states

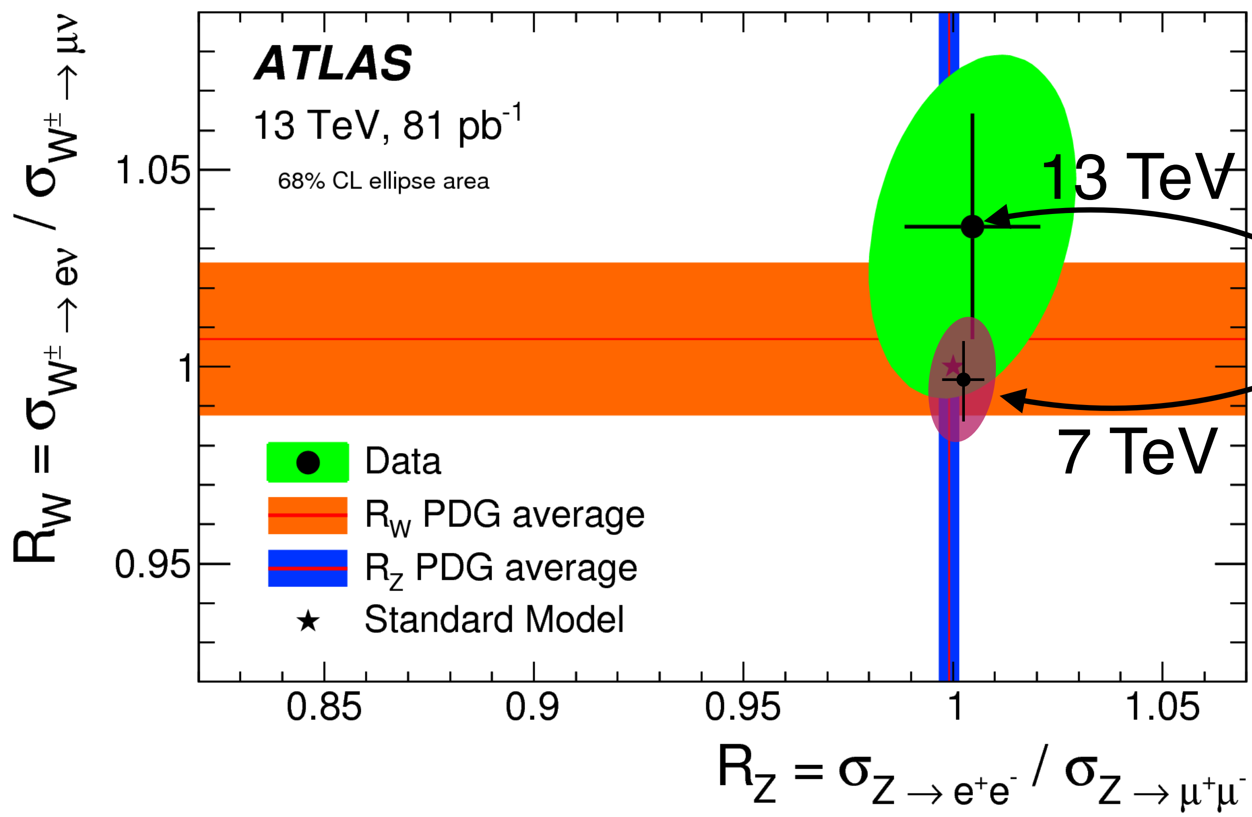

Agreement with NNLO SM predictions

Production cross sections more understood @7 TeV than 13 TeV!

→ see Ksenia Gasnikova's talk

Plenty of room for improvement @13 TeV

- Measurement precision better than predictions ← Simultaneous combination of W^+, W^- and Z fiducial cross sections

Z~1% and W~2% (±2.1% lumi)

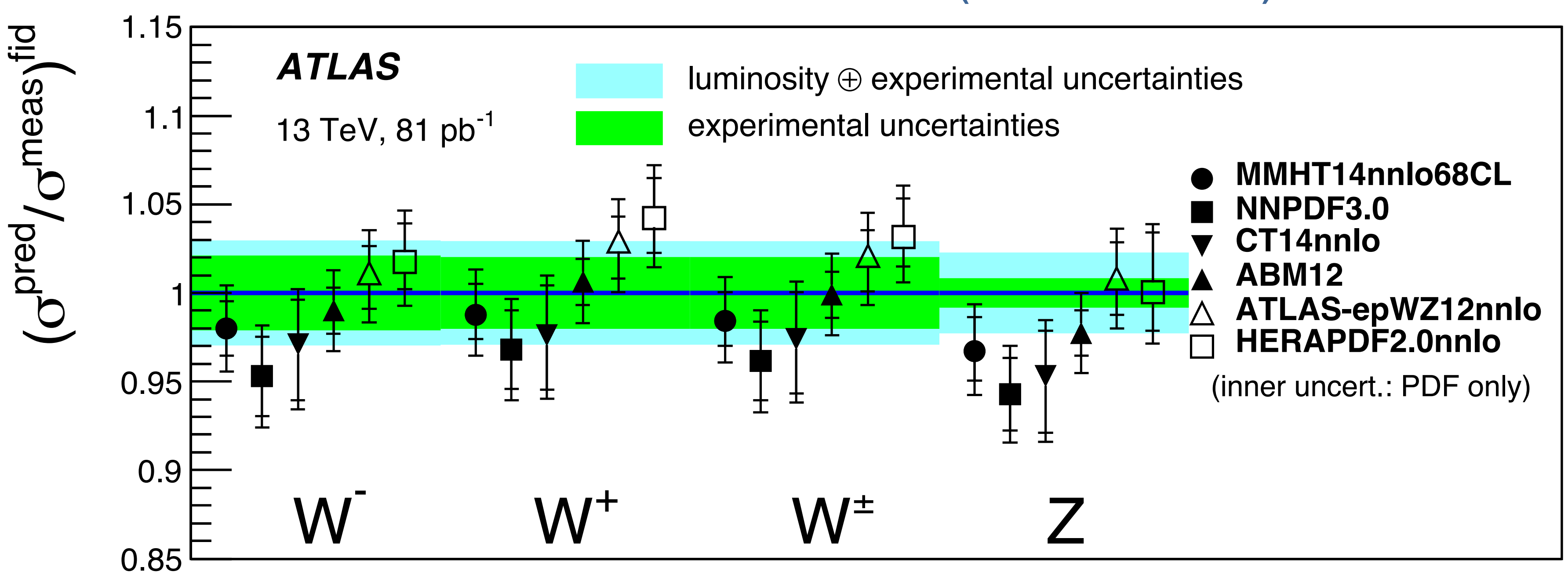

prediction uncertainties dominated by PDFs: ~6% for W± and ~7% for Z

Cross Sections can constrain proton PDFs

W and Z cross sections · Ratios

13 TeV, 81 pb^{-1}

- Ratios benefit from the cancellation of some uncertainties (ex. lumi)

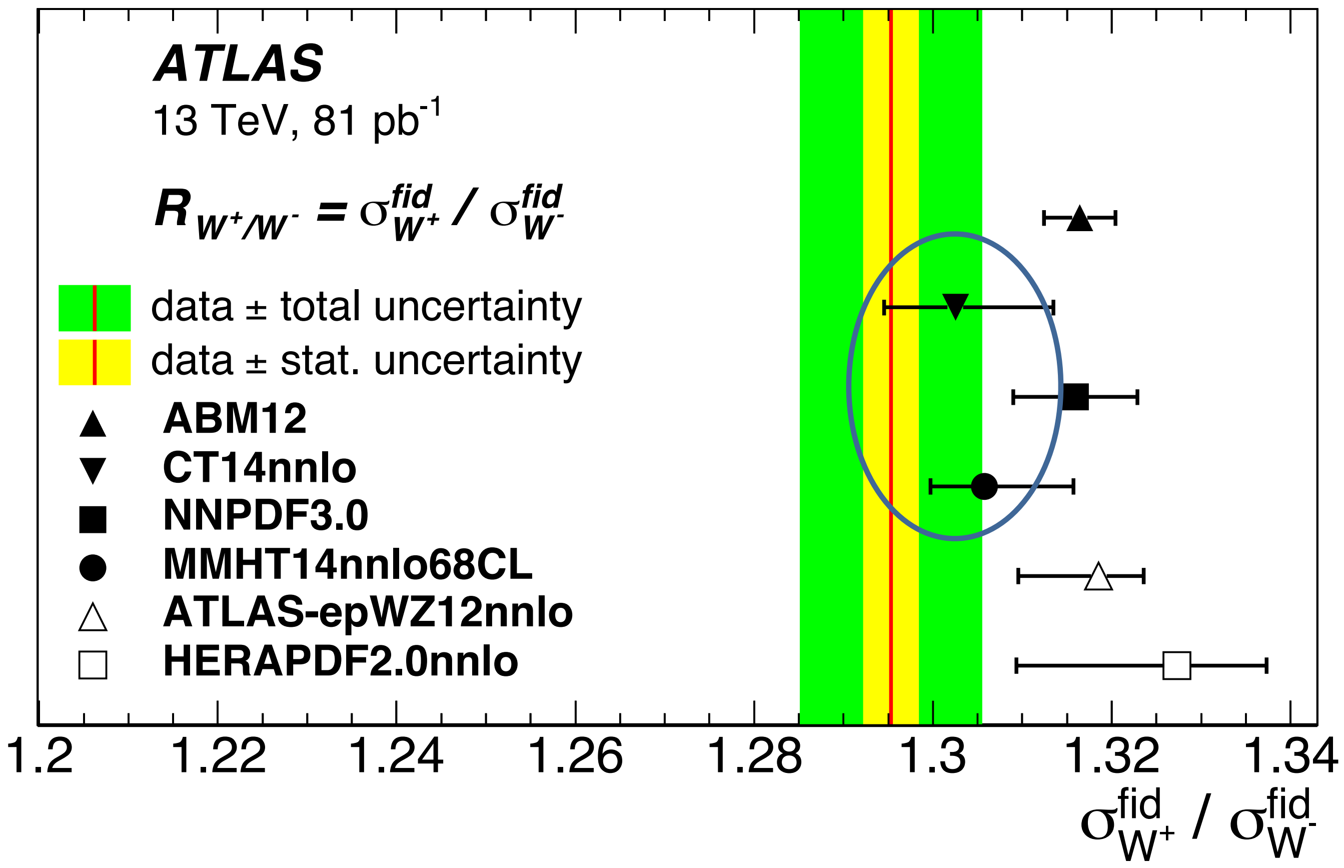

High precision measurement (~0.8%)
→ **discriminate among various PDFs**

W^+/W^- favours CT14nnlo and MMHT14nnlo PDFs

$W^\pm/Z$ compatible with all PDFs within uncertainties

ATLAS-epWZ12 is the most predictive calculation available and it contains fits on ATLAS data.

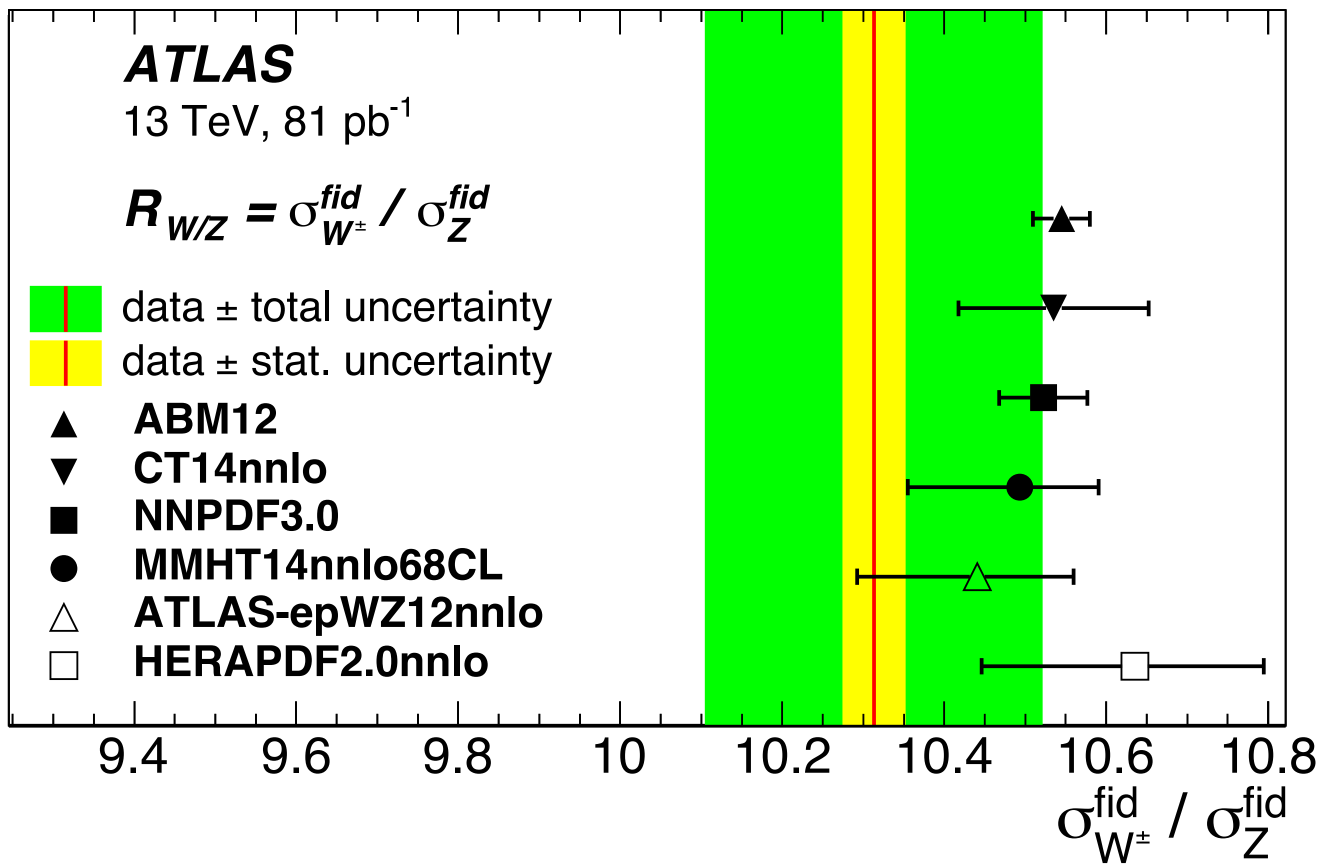

- The W mass is incorporated in the Standard Model through a symmetry breaking mechanism, that relies on the existence of the Higgs boson
- At **LO in EW**, the **W mass** is:

$$m_W^2\left(1-\frac{m_W^2}{m_Z^2}\right)=\frac{\pi\alpha}{\sqrt{2}G_\mu}(1+\Delta r)$$

Δr: radiative NLO corrections to m_W are dominated by top-quark and Higgs loops

→ Δr ∝ m_t^2 and $\ln(m_H)$

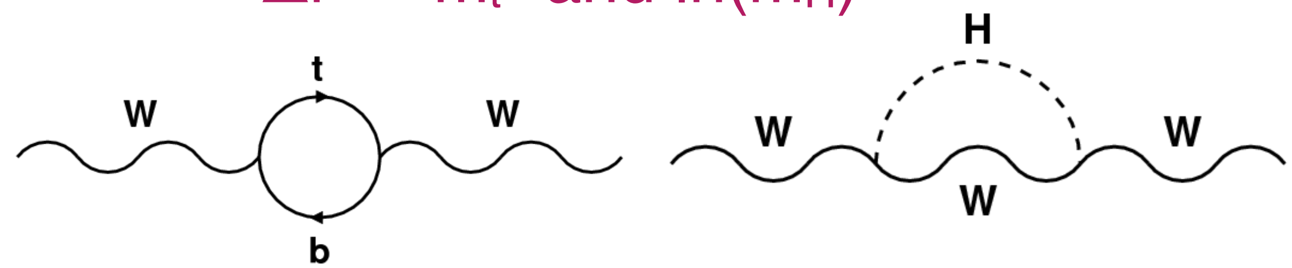

Δr contains contributions from any additional particles and interactions → **probe for BSM**

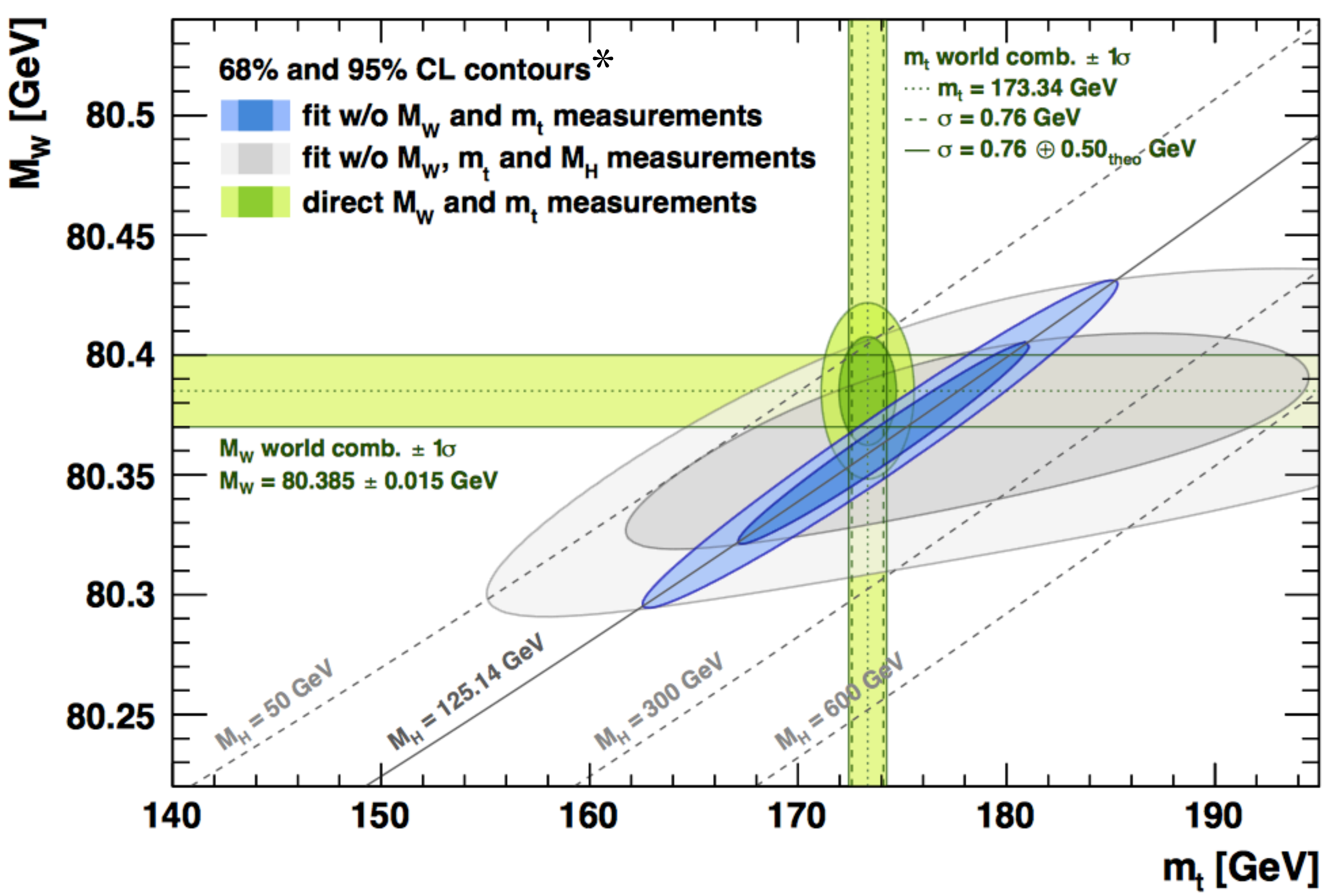

- The relation among m_W, m_t and m_H provides a stringent test of the SM
- m_W is the leading uncertainty in the SM consistency test
- The comparison between the measured value of m_H and the predicted one is sensitive to new physics

Eur. Phys. J. C 74 (2014) 3046

Eur. Phys. J. C 74 (2014) 3046

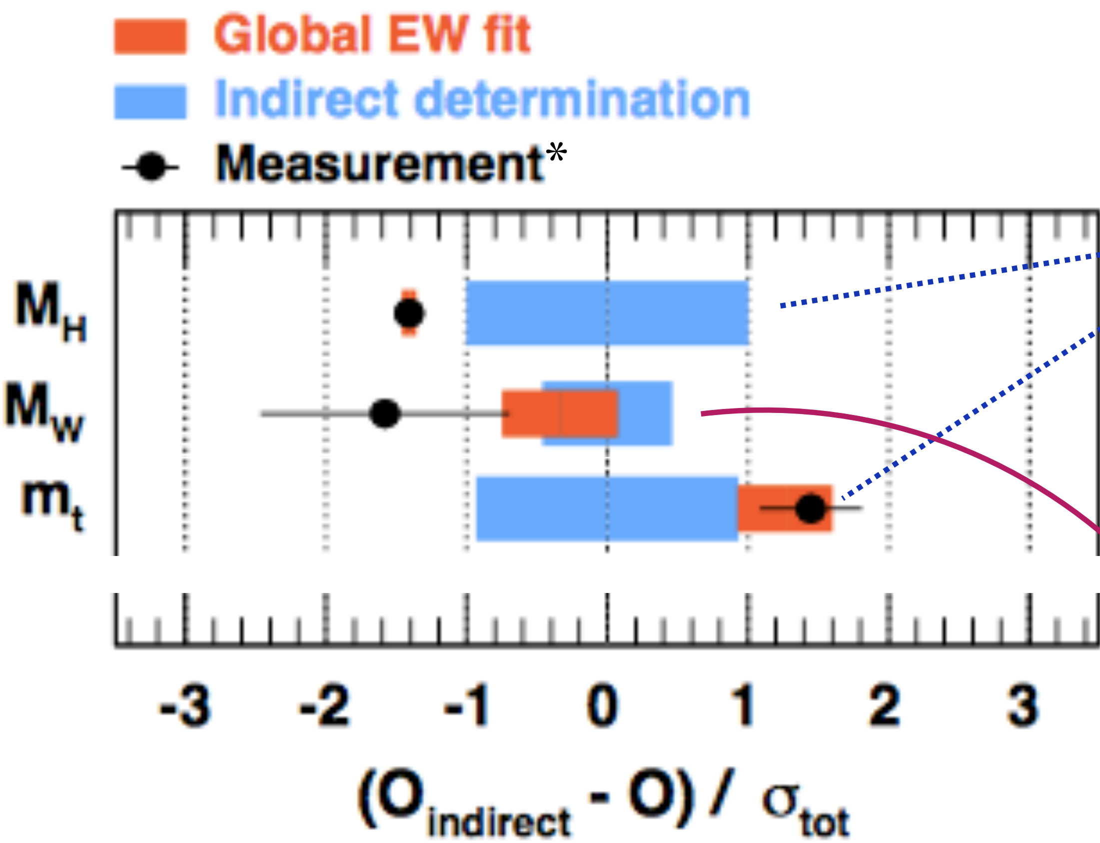

◁ m_H and m_t are more precise than their indirect determination from the global fit

→ improving precision in the measurement will not increase sensitivity to new physics

arXiV:1608.01509

	SM Predictions [GeV]	Measurement [GeV]
m_H	102.8 ± 26.3	125.09 ± 0.24
m_t	176.6 ± 2.5	172.84 ± 0.70
m_W (Tevatron)	80.360 ± 0.008	80.385 ± 0.015

✤ the indirect determination of the W mass is more precise (± 8 MeV) than measurements

→ improving the precision of the W mass is necessary to increase the sensitivity of the global fit to new physics

Challenging environment @LHC:

◁ second generation of quark PDFs play a larger role ~25% W production (5% at Tevatron)

◁ implication in the p_T^W distributions
→ additional uncertainty on PDFs
→ larger uncertainty due to W-polarisation affecting the p_T^{lep} distribution
→ larger production of W from gluons

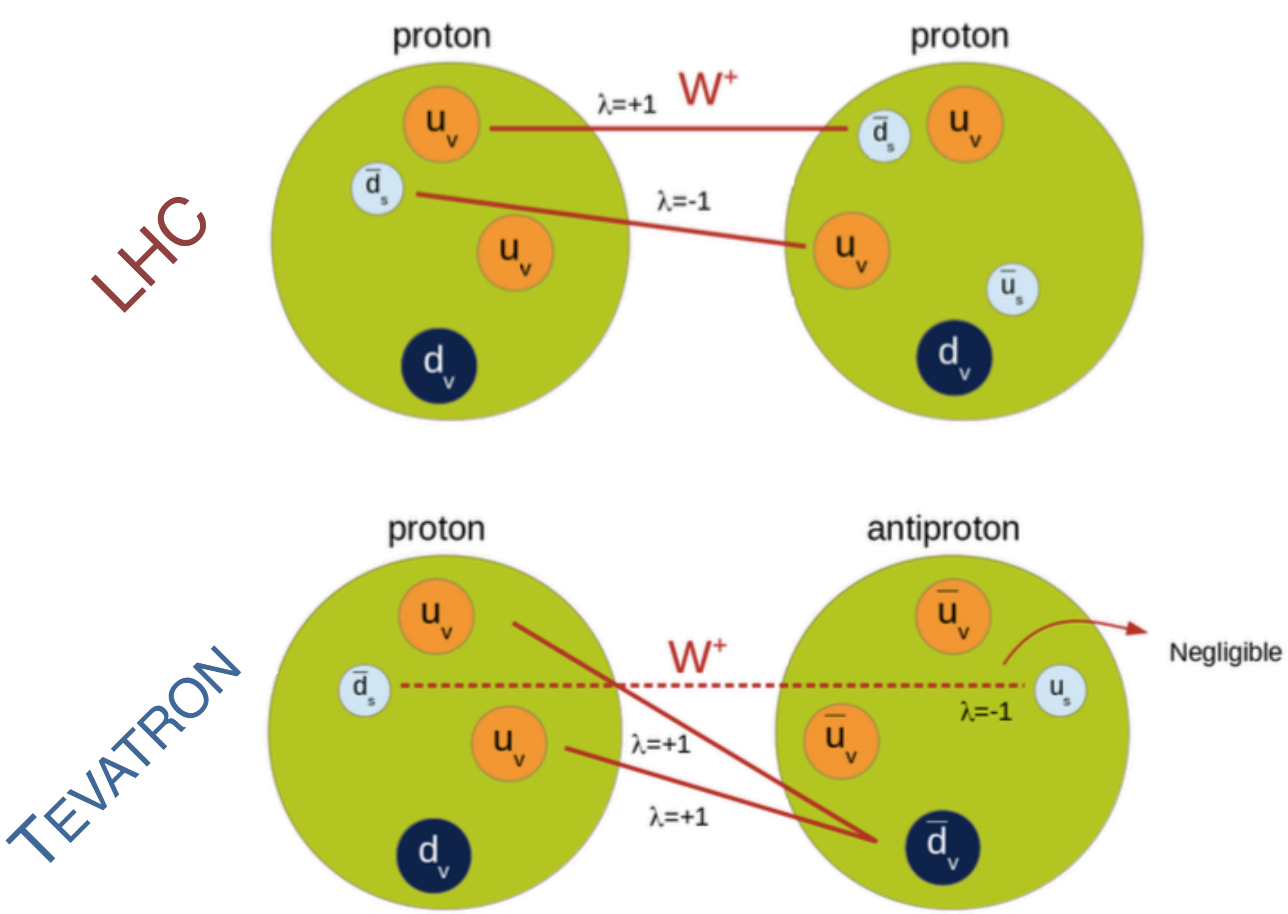

LEP+Tevatron: M_W unc. ~15 MeV
Best individual measurement from CDF: M_W unc. ~19 MeV

*Phys.Rev. D88 (2013) no.5, 052018

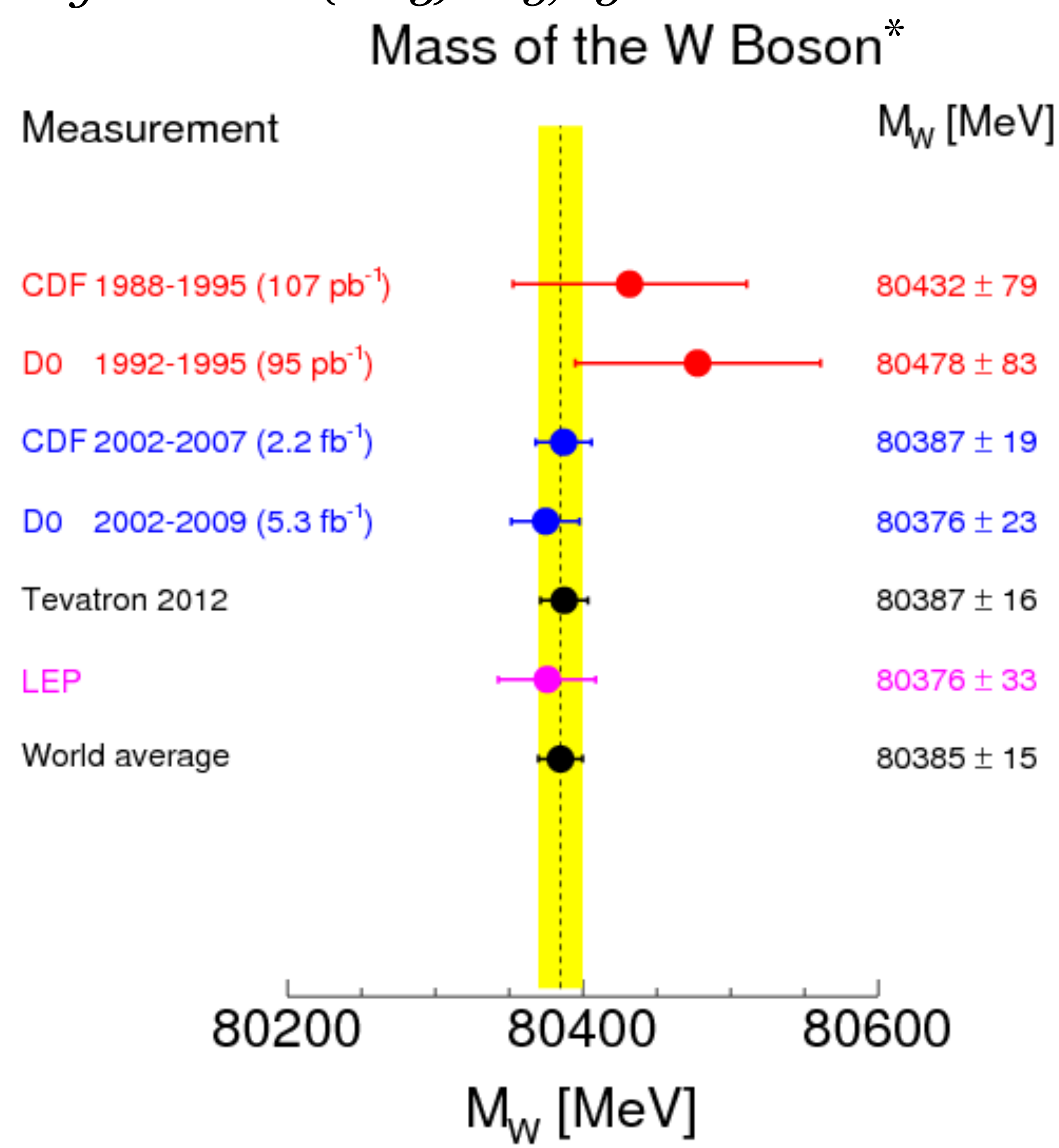

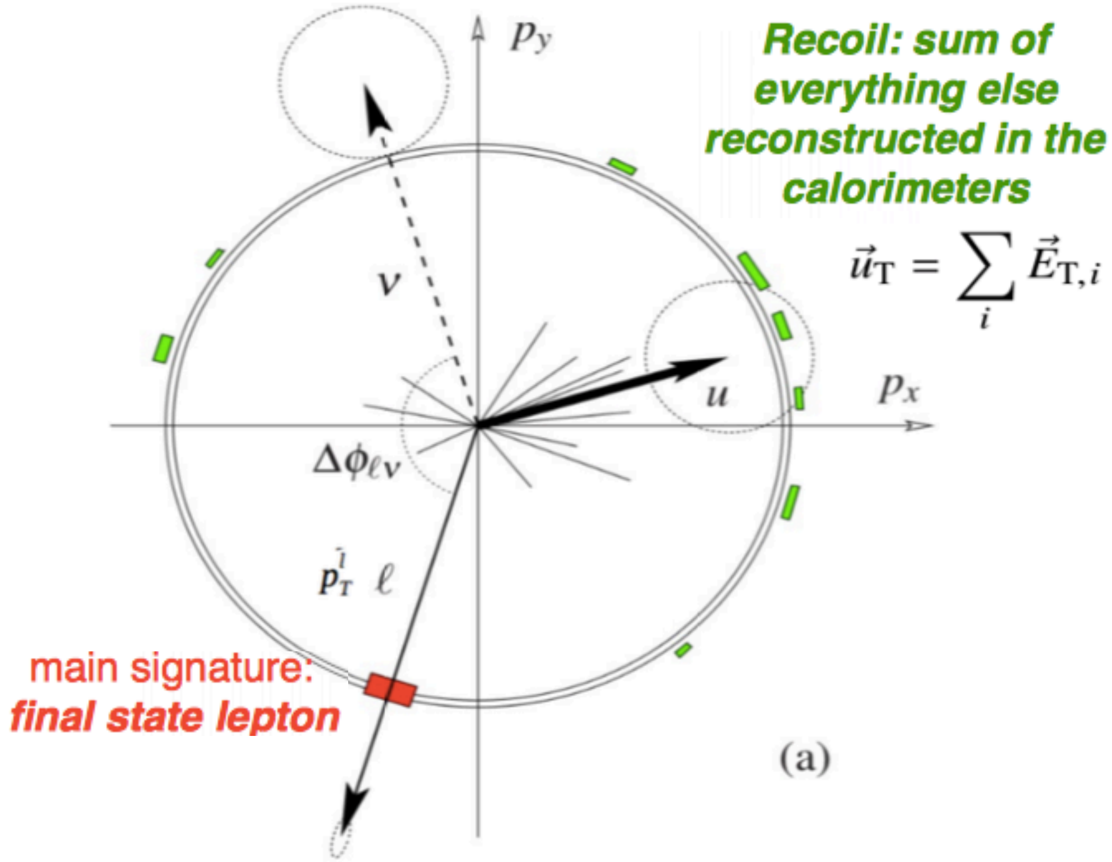

- Important components: charged lepton and recoil to reconstruct p_T^ν
- **m_W from fits on p_T^{lep} and m_T^W templates generated for different values of m_W**
  → χ^2 minimisation gives the best fit template
  ◁ templates simulated for different values of m_W, obtained by reweighing m_W according to the Breit-Wigner

- Coherent and exhaustive description of the Drell-Yan production mechanism
  → Physics Modelling

Slide 19

- Detector calibration and strategy validation on Z→ll events
  ◁ use Z→ll events to calibrate leptons and recoil
    → test reco+id+trigger efficiencies on p_T^{lep} (impact on templates)
  ◁ m_Z is calculated with the same strategy of the W mass
  ◁ extrapolation from Z to W→ additional systematic

- m_W extract 28 different categories and combined
  → validate calibrations, modelling and improve accuracy

Slide 22

- **Drell-Yan cross section** can be factorised as:

$$\frac{d\sigma}{dp_1 dp_2} = \underbrace{\left[\frac{d\sigma(m)}{dm}\right]}_{\text{Breit-Wigner}} \overbrace{\left[\frac{d\sigma(y)}{dy}\right]}^{\text{NNLO pQCD}} \underbrace{\left[\frac{d\sigma(p_T,y)}{dp_T dy}\left(\frac{d\sigma(y)}{dy}\right)^{-1}\right]}_{\text{Parton Shower}} \left[(1+cos^2\theta) + \overbrace{\sum_{1=0}^{7}}^{\text{NNLO pQCD}} A_i(p_T,y)P_i(cos\theta,\phi)\right]$$

- the factorisation allows to use the **most appropriate model for each part**
- m_W from template fit of p_T^{lep} and m_T^W distributions
  → calls for precise templates (and mw-dependence) predictions

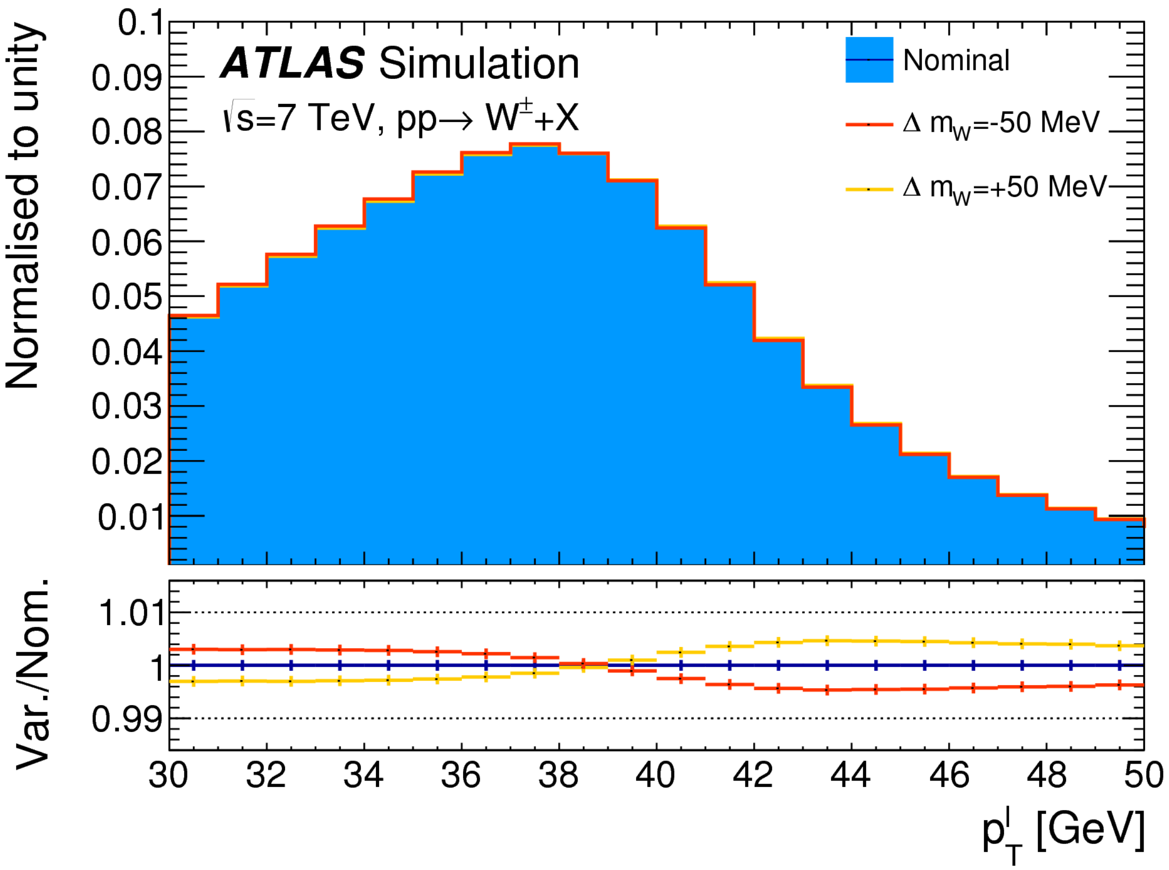

large uncertainties on p_T^{lep}

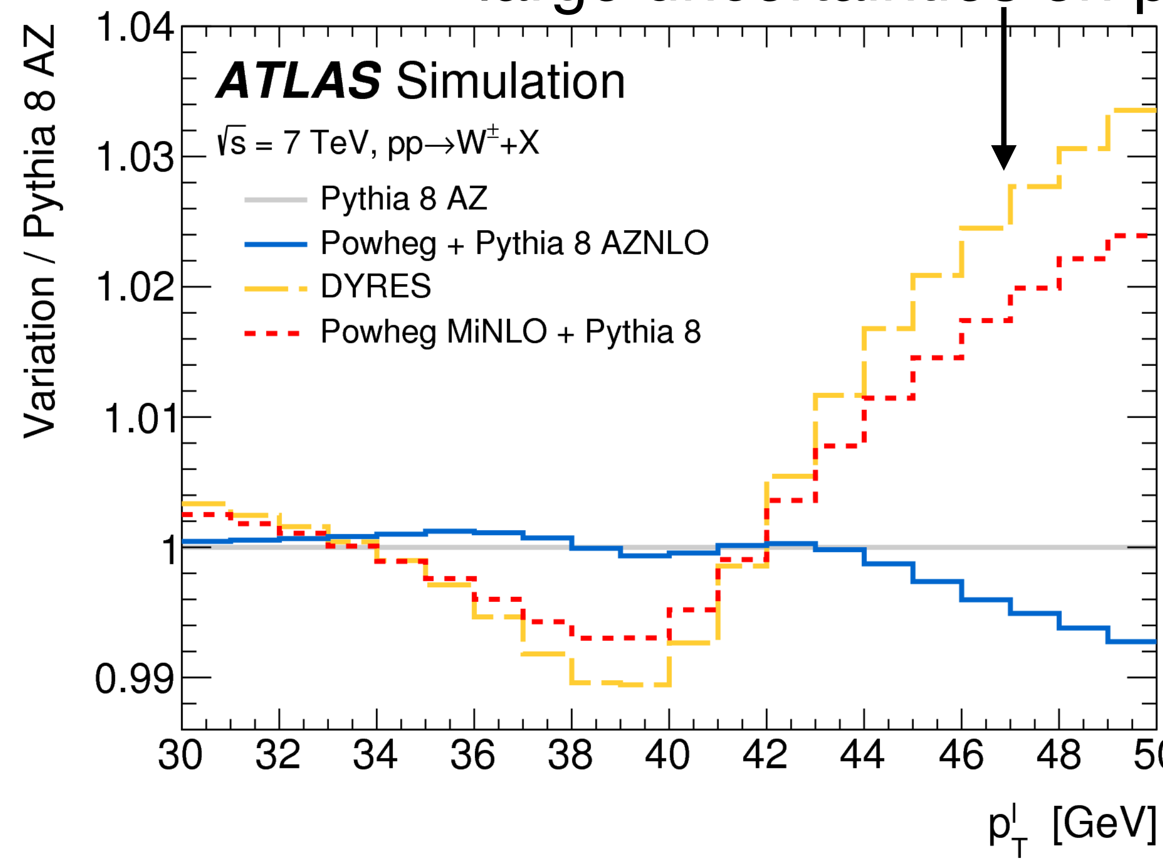

✤ Ancillary Drell-Yan measurements to validate and constrain the modelling:

1) PDFs + dσ/dy → **W/Z measurements @ 7 TeV** (see Ksenia Gasnikova's talk)

2) QCD parameter to Parton Shower → **fits on p_T^Z distribution @ 7 TeV**

Comparison of Pythia 8 AZ and 4C predictions to the p_T^Z distribution with data used to determine the AZ tune

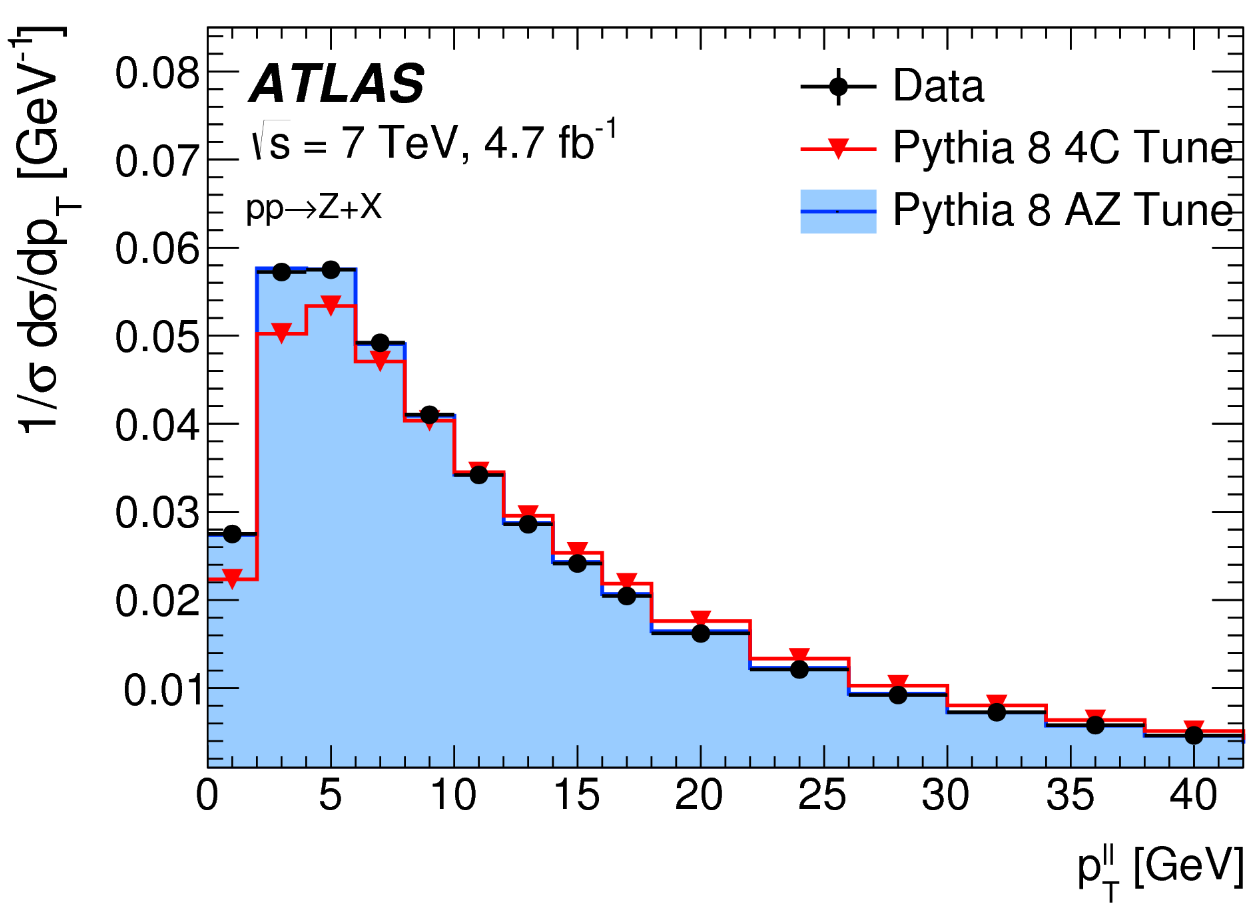

3) A_i angular coefficients → **comparison of theoretical predictions with measurements @ 8 TeV**

A_0-A_2 non-zero only at NNLO QCD predictions

*JHEP08 (2016) 159

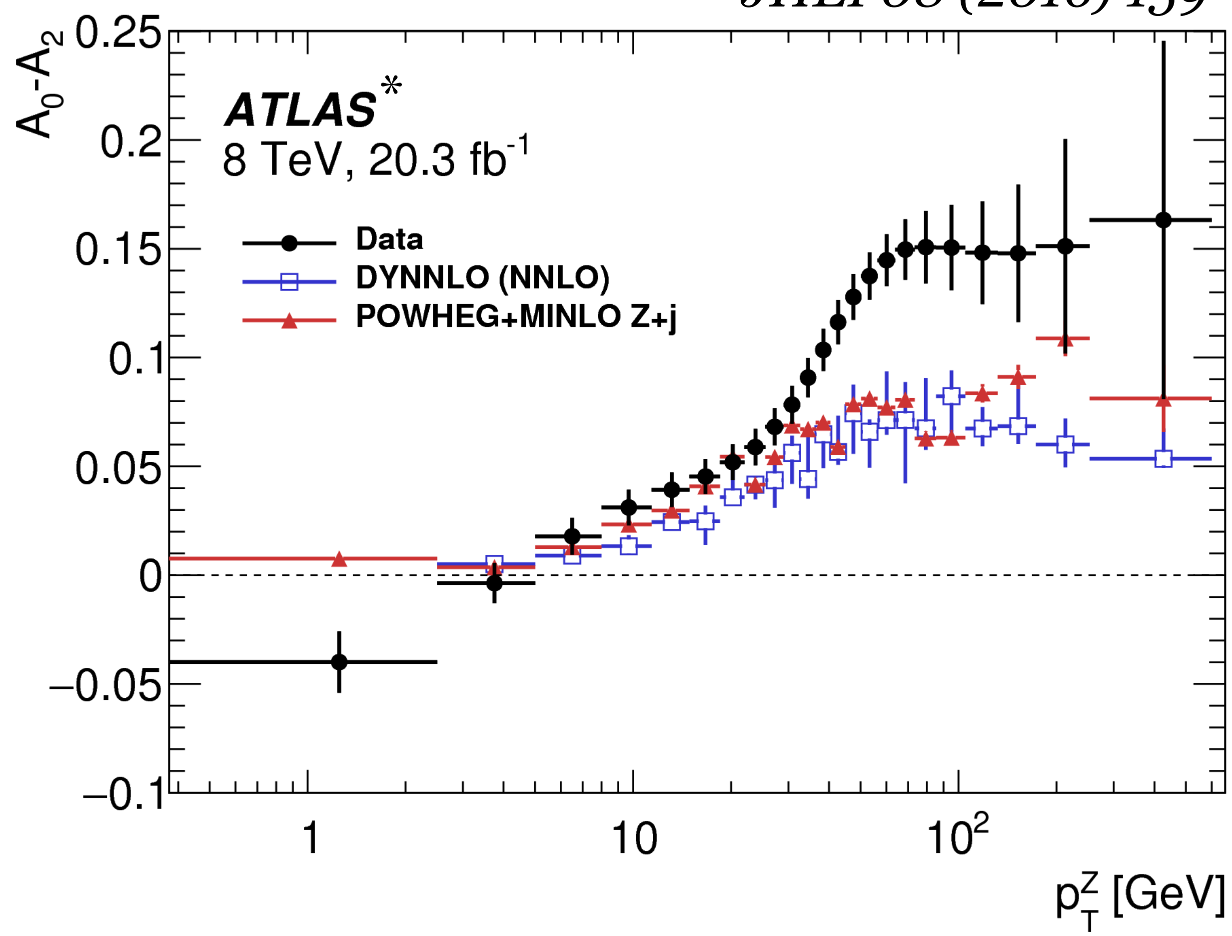

✤ EW corrections

Dominant contribution from QED FSR

Decay channel	$W \to e\nu$		$W \to \mu\nu$	
Kinematic distribution	p_T^ℓ	m_T	p_T^ℓ	m_T
δm_W [MeV]				
FSR (real)	< 0.1	< 0.1	< 0.1	< 0.1
Pure weak and IFI corrections	3.3	2.5	3.5	2.5
FSR (pair production)	3.6	0.8	4.4	0.8
Total	4.9	2.6	5.6	2.6

◁ larger impact in p_T^{lep} than in m_T^W

◁ similar contributions in electron and muon channels

✤ QCD corrections

PDFs are the dominant uncertainty, followed by variations on p_T^W due to heavy-quarks in the initial state

W-boson charge	W^+		W^-		Combined	
Kinematic distribution	p_T^ℓ	m_T	p_T^ℓ	m_T	p_T^ℓ	m_T
δm_W [MeV]						
Fixed-order PDF uncertainty	13.1	14.9	12.0	14.2	8.0	8.7
AZ tune	3.0	3.4	3.0	3.4	3.0	3.4
Charm-quark mass	1.2	1.5	1.2	1.5	1.2	1.5
Parton shower μ_F with heavy-flavour decorrelation	5.0	6.9	5.0	6.9	5.0	6.9
Parton shower PDF uncertainty	3.6	4.0	2.6	2.4	1.0	1.6
Angular coefficients	5.8	5.3	5.8	5.3	5.8	5.3
Total	15.9	18.1	14.8	17.2	11.6	12.9

◁ PDFs anti correlated between W^+ and W^- and reduced by combination

◁ similar contributions from p_T^{lep} and m_T^W

- Same strategy performed in 28 different categories in p_T^{lep}, m_T^W and η^{lep} among electron and muon channels

◁ consistent m_W extraction in all categories

→ strong validation of physics modelling and calibrations

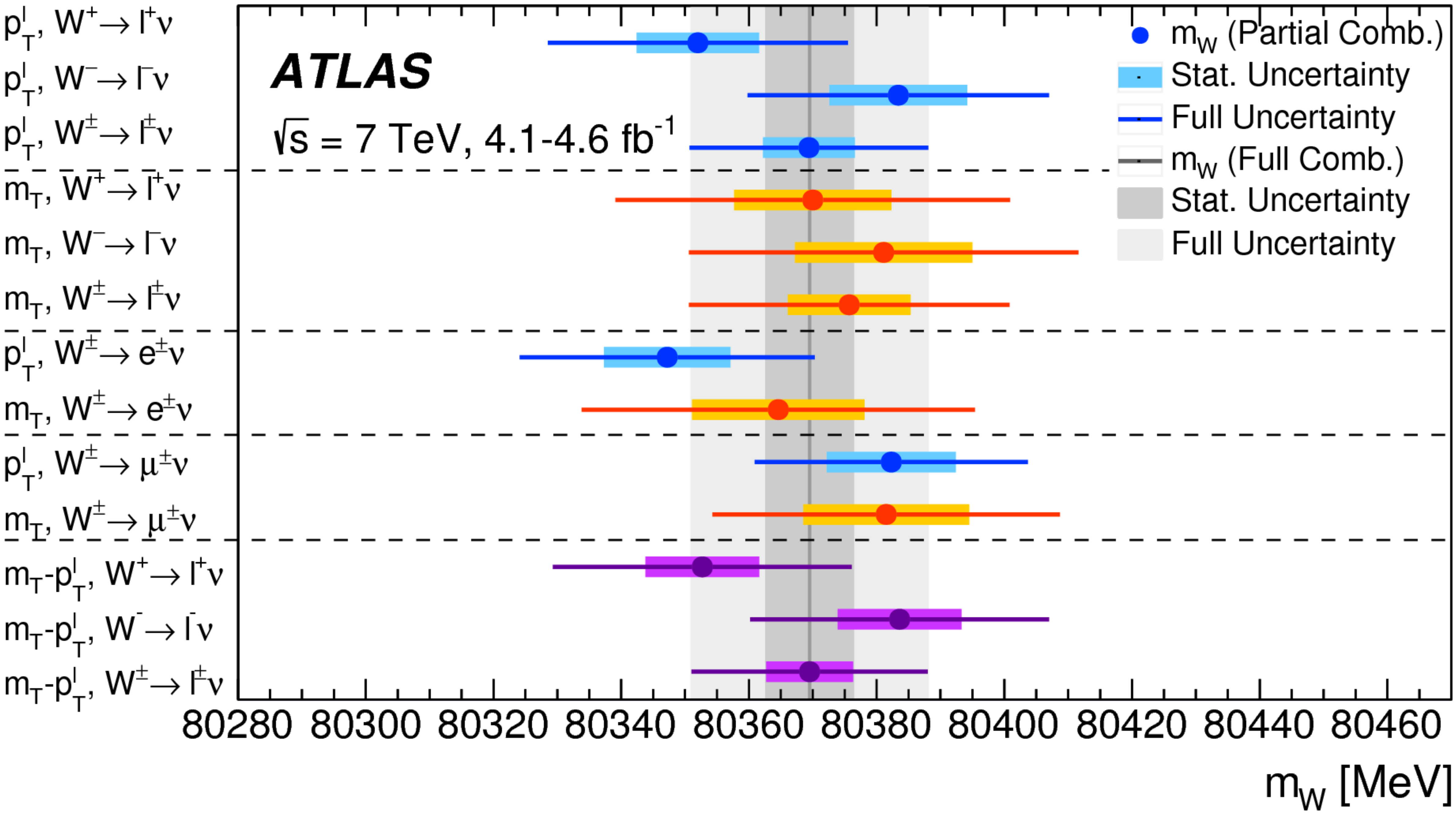

W mass · Results

m_W = 80369.5 ± 6.8 (stat.) ± 10.6 (syst.) ± 13.6 (mod.) MeV

80369.5 ± 18.5 MeV

The uncertainty is dominated by theoretical modelling, with largest contribution from PDF and QCD

Combined categories	Value [MeV]	Stat. Unc.	Muon Unc.	Elec. Unc.	Recoil Unc.	Bkg. Unc.	QCD Unc.	EWK Unc.	PDF Unc.	Total Unc.
m_T, p_T^l, $W^\pm$, e-μ	80369.5	6.8	6.6	6.4	2.9	4.5	8.3	5.5	9.2	18.5

Result consistent with SM, compatible with the world average and competitive with CDF measurements

Tension between SM prediction and measurement reduced with respect to Tevatron results

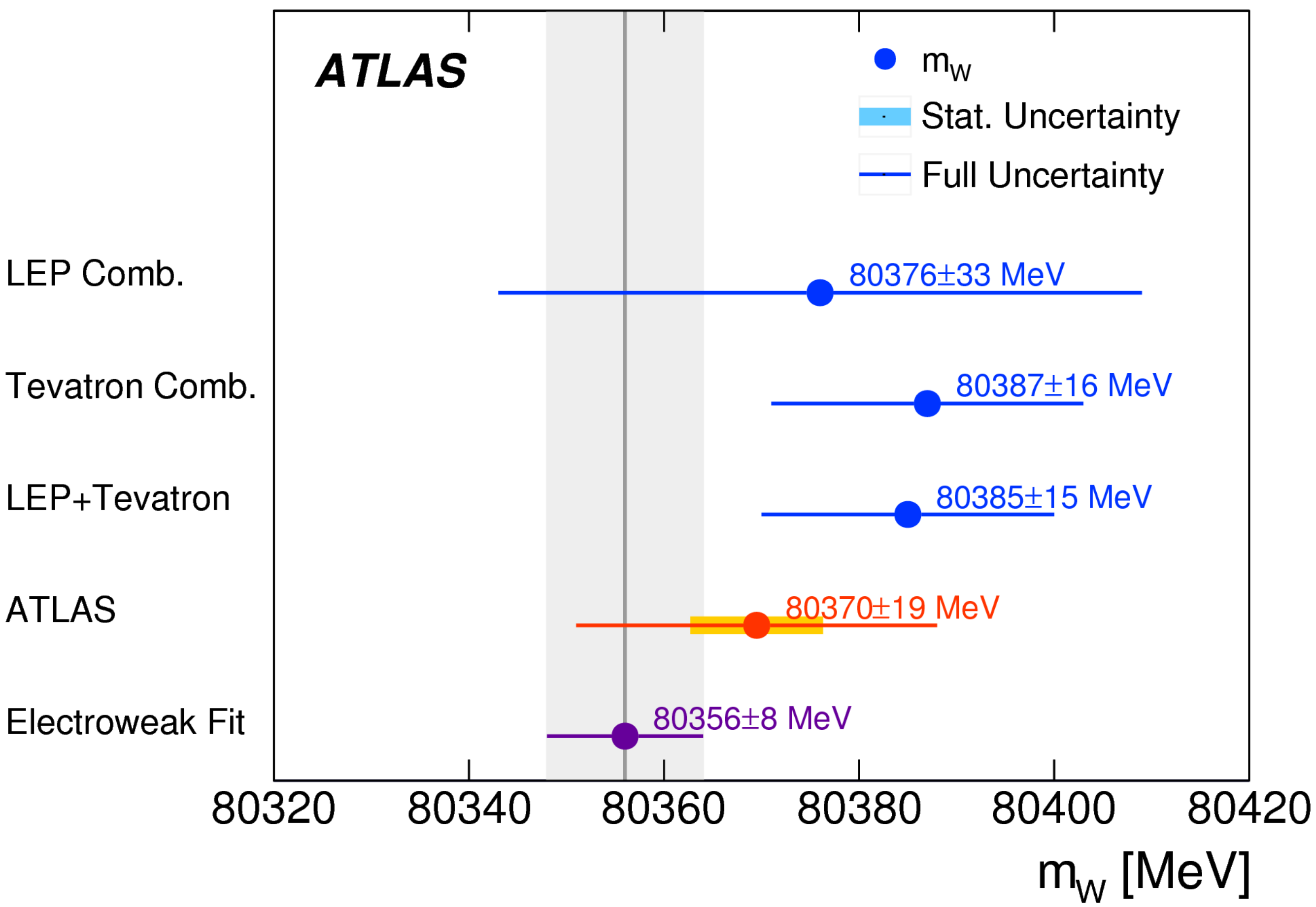

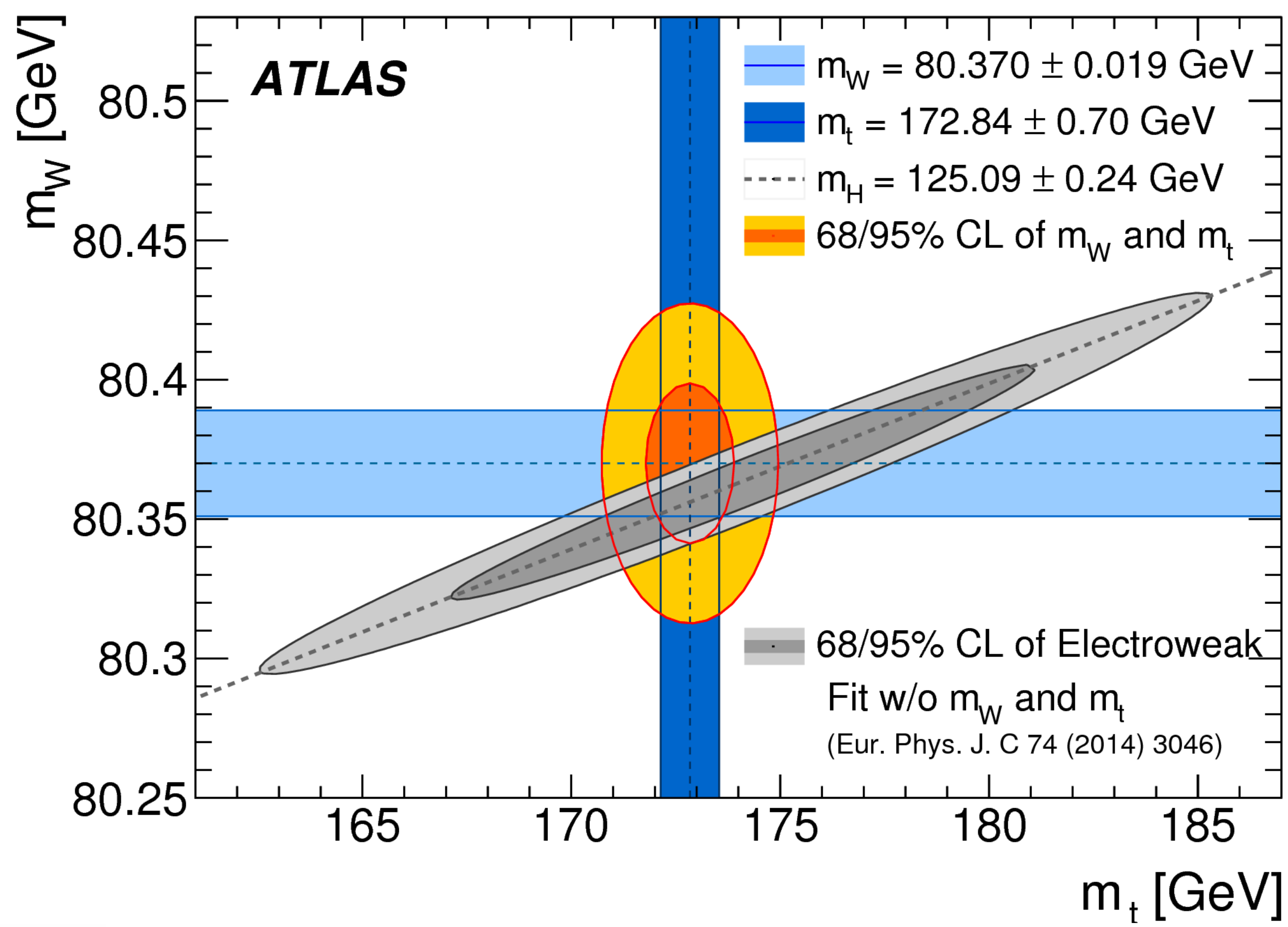

Conclusions

W/Z processes @ LHC allow precise measurements of EW parameters

- Unique measurement of the 3D Z cross section @ 8 TeV
  - In the Z-peak region, data accuracy better than 0.5%
  - A_{FB} is mainly due to the Z/ɣ* interference changes sign at m_Z
  - The results are well described by predictions

$$\frac{d^3\sigma}{dm_{ll}dy_{ll}dcos\theta^*}$$

- Tau polarisation in Z→$\tau\tau$ events @ 8 TeV
  - from fit on ϒ based on the kinematics of hadronic visible decays
  - fiducial results are extrapolated to $66<m_{Z/\gamma^*}<116$ GeV and are in agreement with SM

- W and Z cross sections and ratios @ 13 TeV
  - at the % level in agreement with NNLO calculations
  - W^+/W^- precision ~0.8% → discriminate among PDFs
  - Plenty of room for improvement!

- First measurement of W mass @ 7 TeV, milestone of LHC program
  - consistent with SM and the current world average value, competitive with CDF
  - uncertainty dominated by theoretical modelling (PDFs and QCD)

→ future benefit in m_T^W resolution and modelling including W/Z measurements @8 and 13 TeV

$$m_W = (80369.5 \pm 18.5)\ \text{MeV}$$

Thanks for your attention!

Extra Slides

3D Cross Section

8 TeV, 20.2 fb^{-1}

◁ A_{FB}<0 below the Z peak, vanishing at m_{ll}~m_Z

◁ cross section for large $\cos\vartheta^*_{CS}$ increases with mass → reduced impact of fiducial cuts

A_{FB}<0

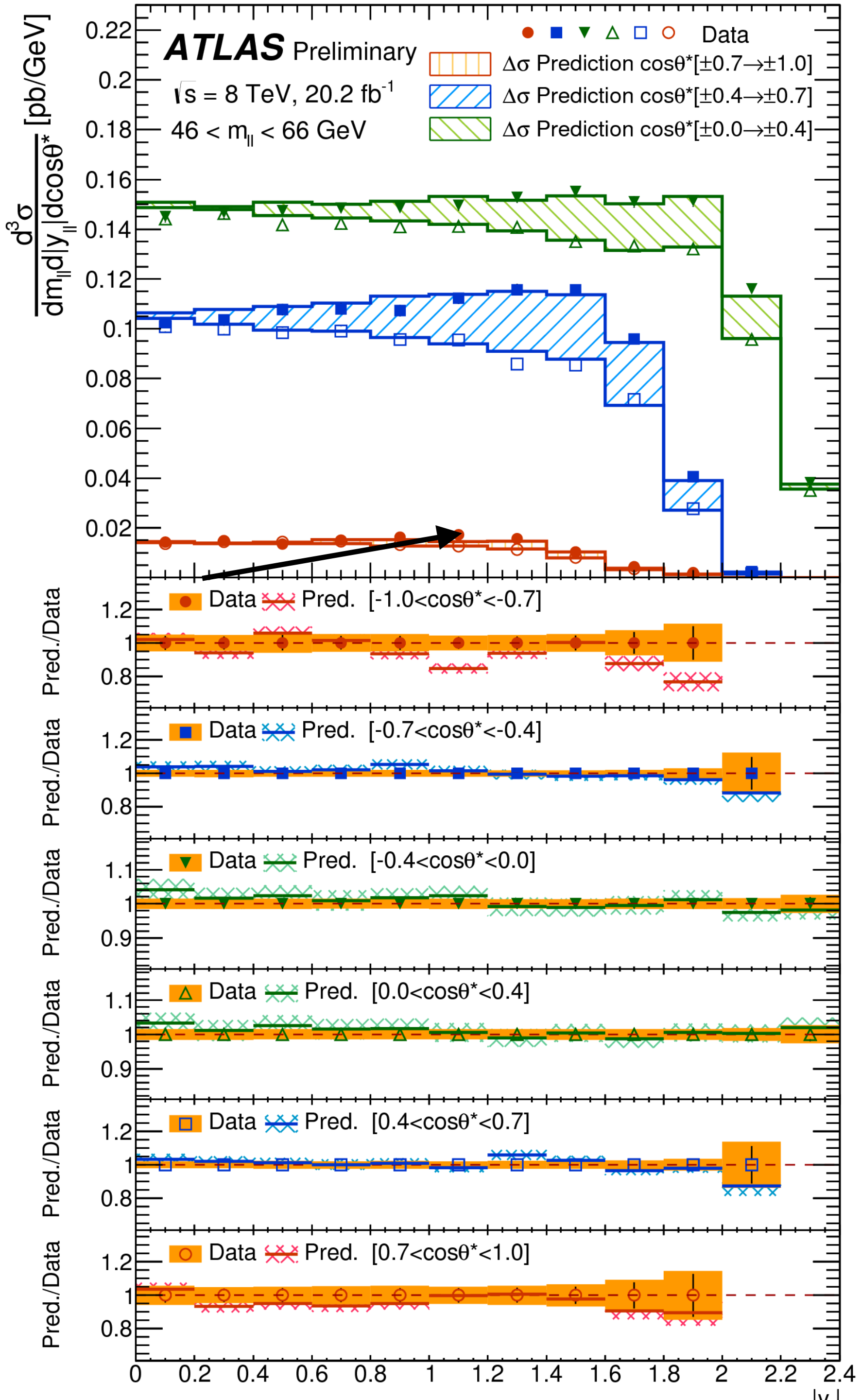

A_{FB}<0

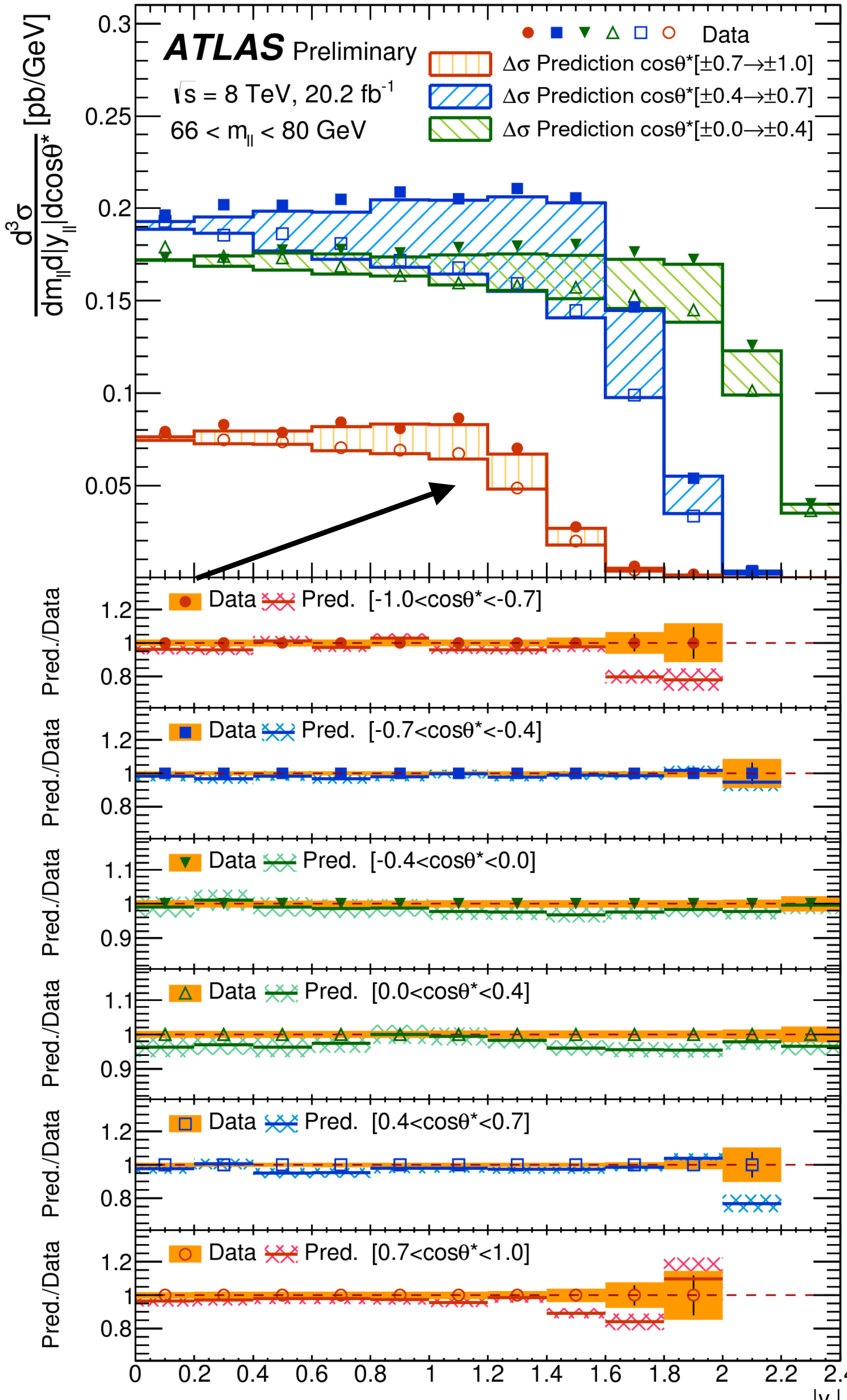

A_{FB}=0

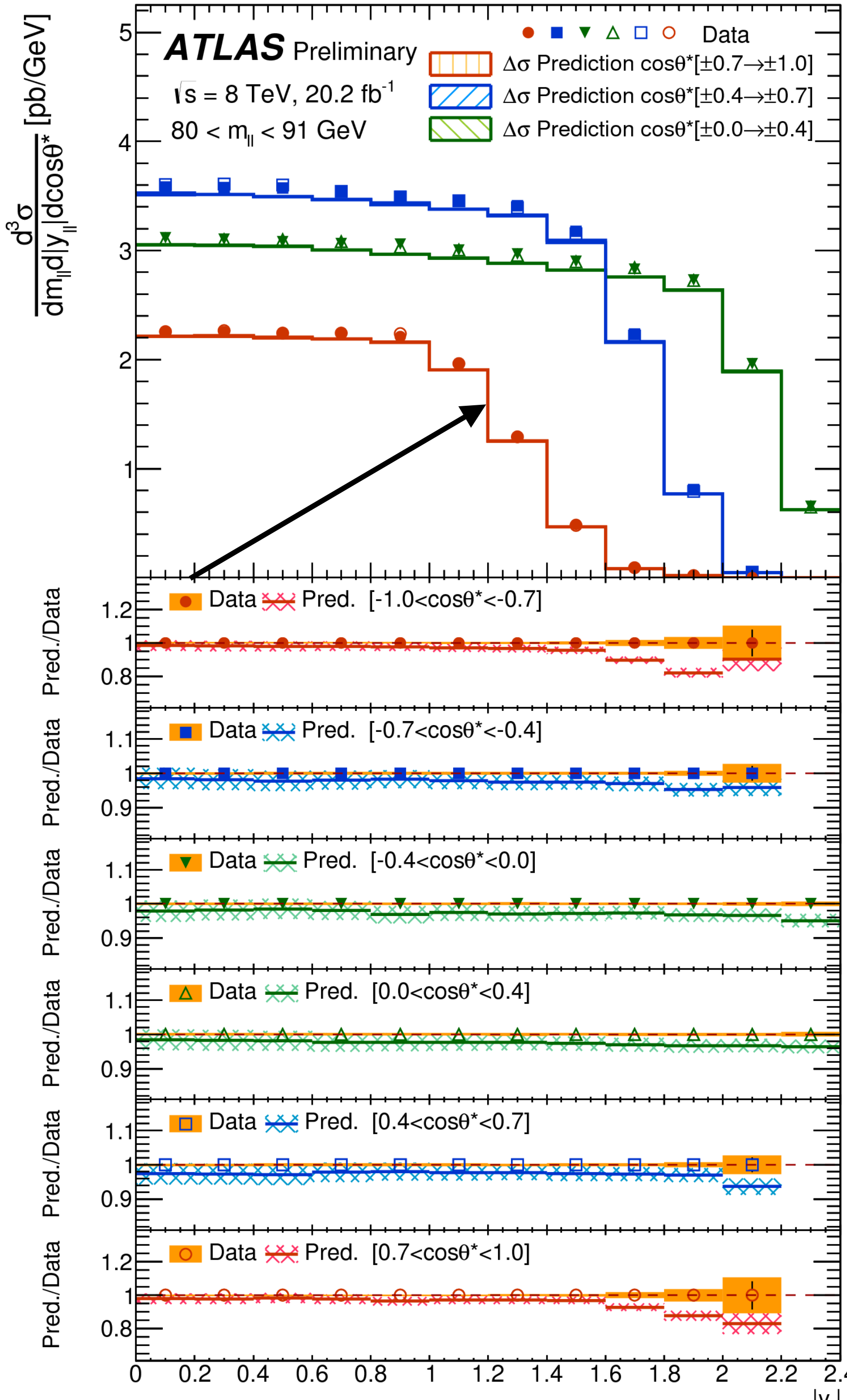

◁ At large y_{ll}, cross sections for $\cos\vartheta^*_{CS}$<0 are 35% larger then for $\cos\vartheta^*_{CS}$>0

3D Cross Section

8 TeV, 20.2 fb^{-1}

- AFB>0 above the Z peak, increasing with m_{ll}
- data precision <0.5% in the Z-peak region for $|y_{ll}|$<1.4

AFB≥0

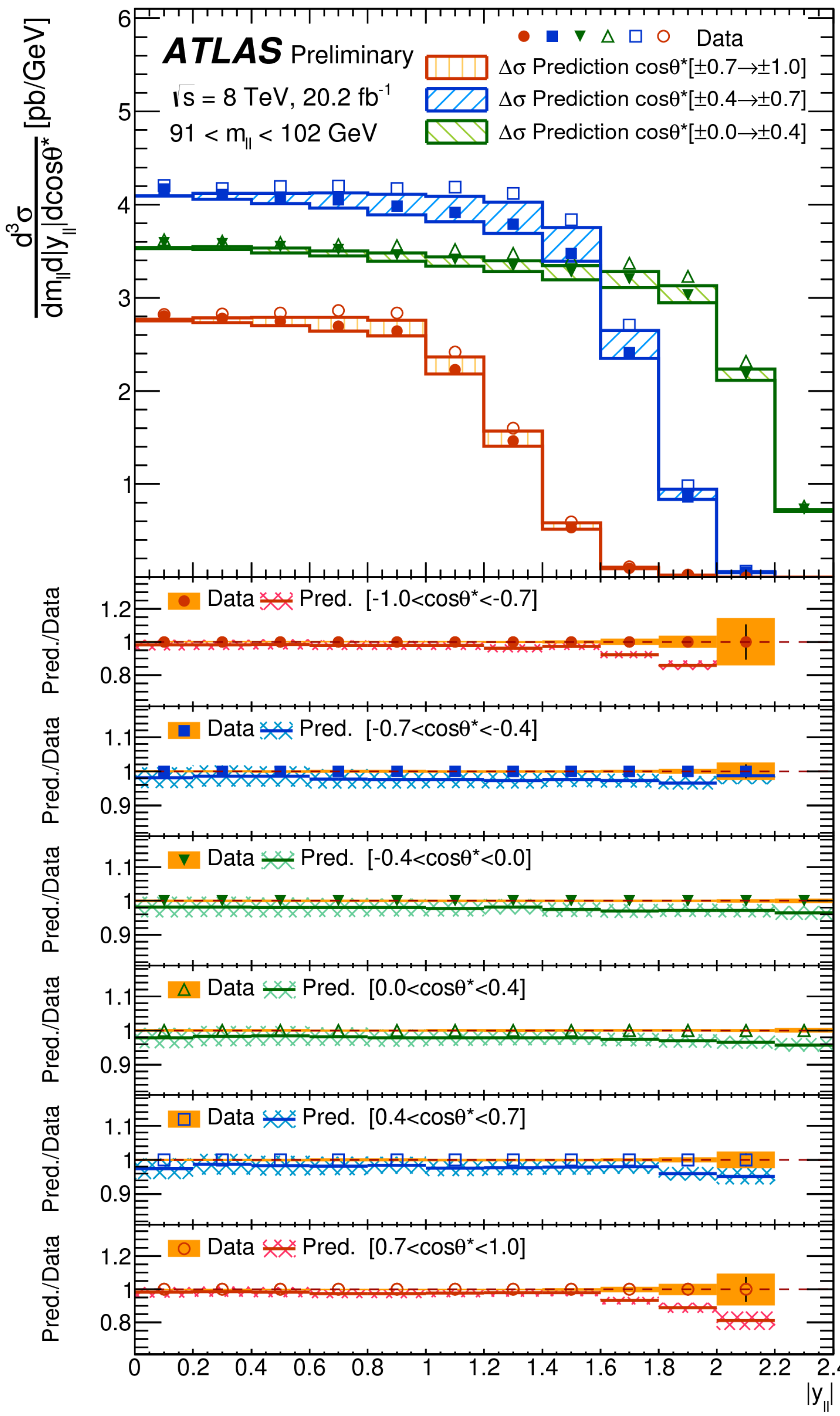

AFB>0

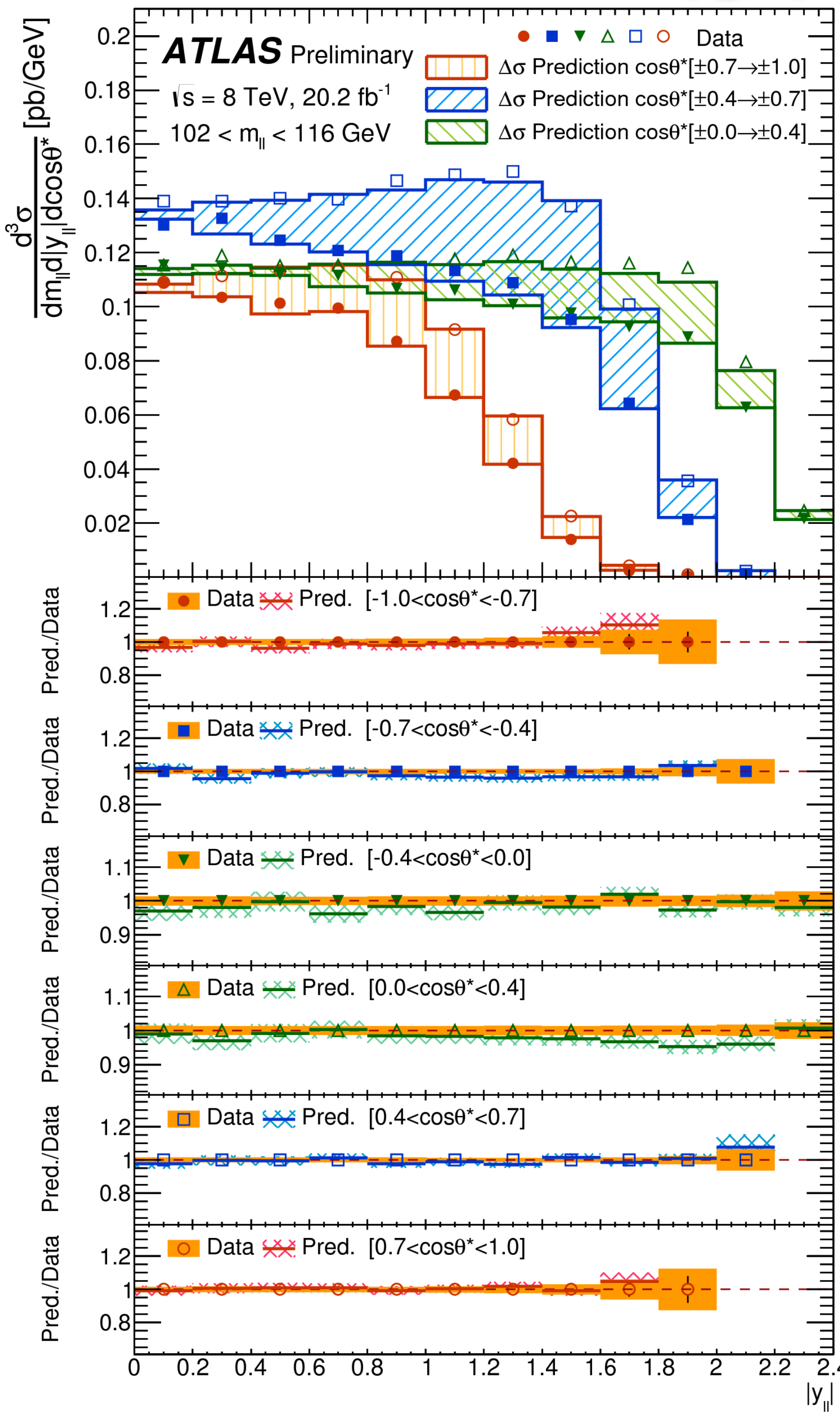

AFB>0

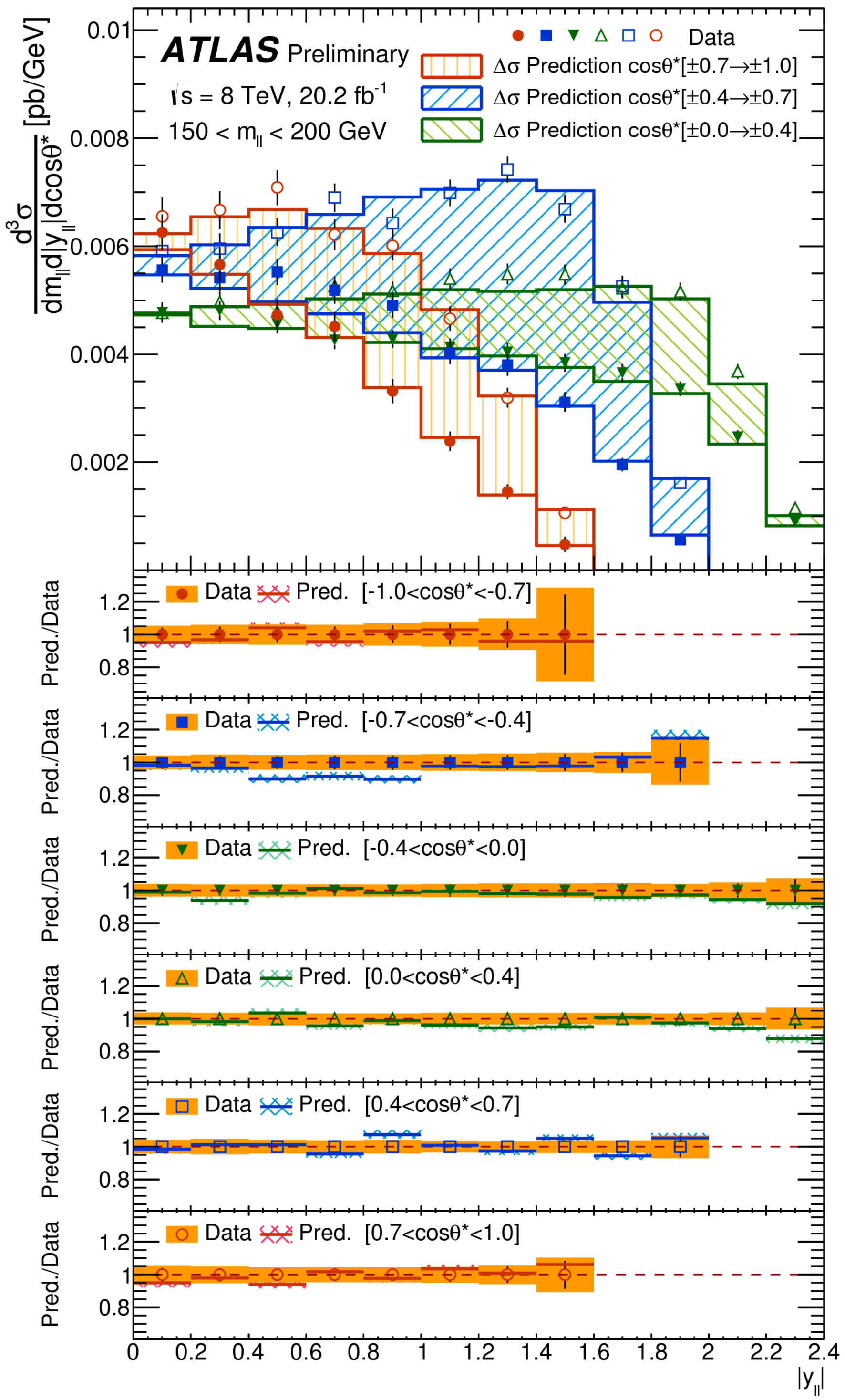

3D Cross Section · A_{FB} in forward region 8 TeV, 20.2 fb^{-1}

◁ measurement more sensitive to A_{FB} at high $|y_{ll}|$ because of more important cancellation of $\cos\vartheta^{*}_{CS}$ symmetric uncertainties

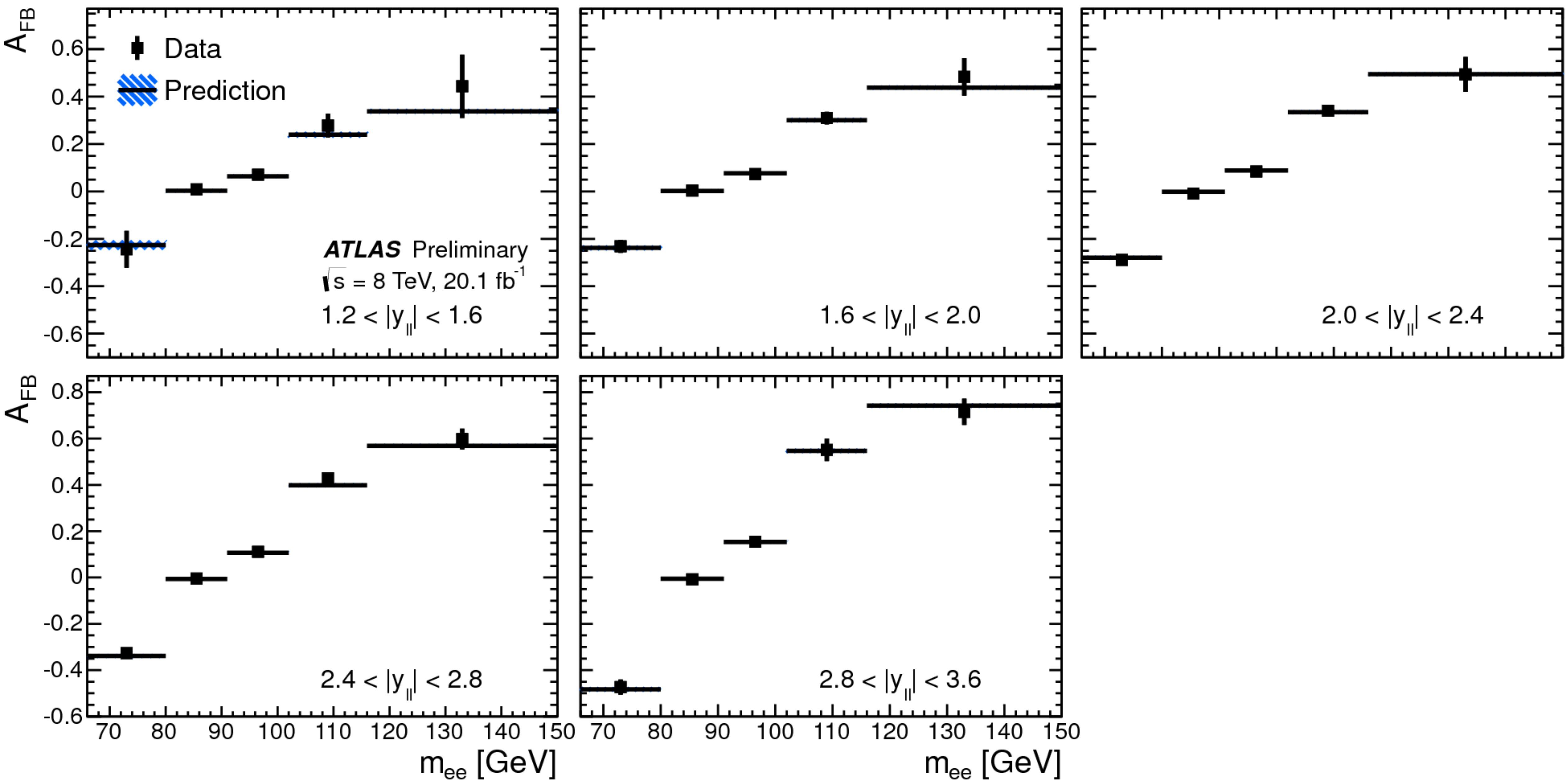

◁ A_{FB} ranges from -0.2 to +0.5 at the lowest and from -0.4 to +0.7 at the largest y_{ll}, in agreement with expectations.

W and Z cross sections 13 TeV, 81 pb^{-1}

Phys. Lett. B 759 (2016) 601

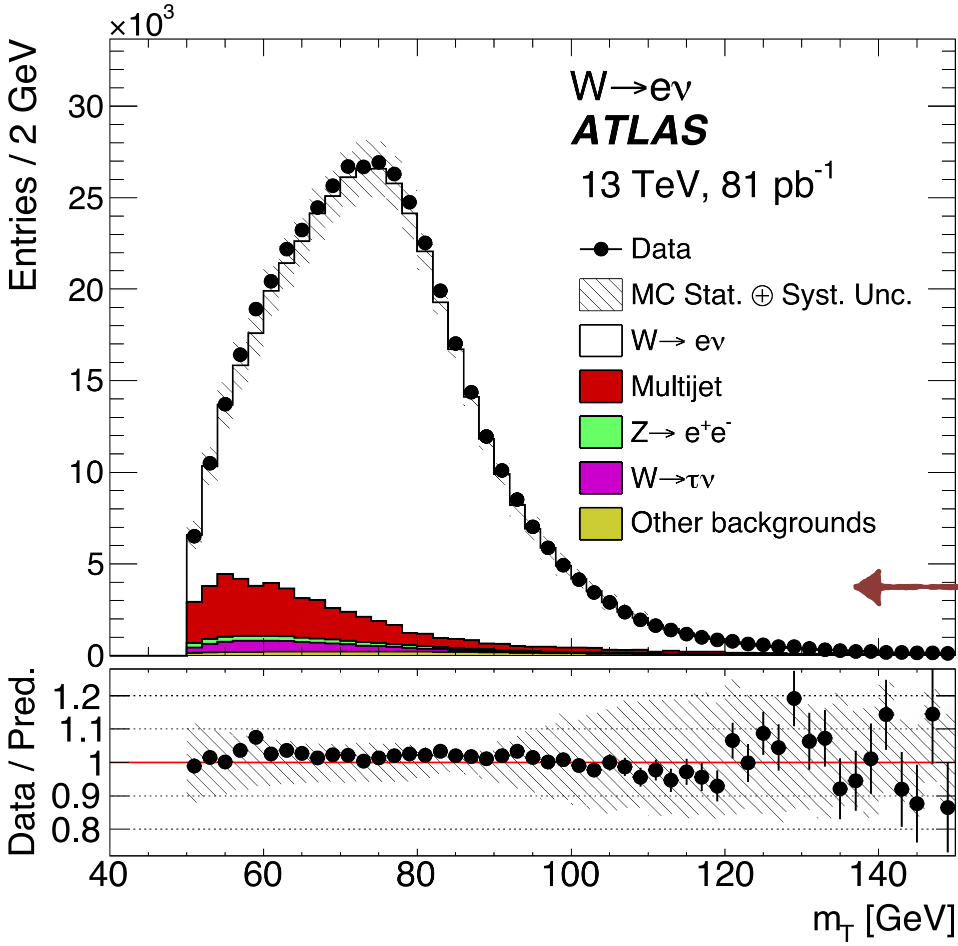

Fiducial Phase Space

$p_T^l > 25$ GeV
$p_T^\nu > 25$ GeV
$|\eta^l| < 2.5$

$m_T^W > 50$ GeV
66 GeV < m_{ll} < 116 GeV

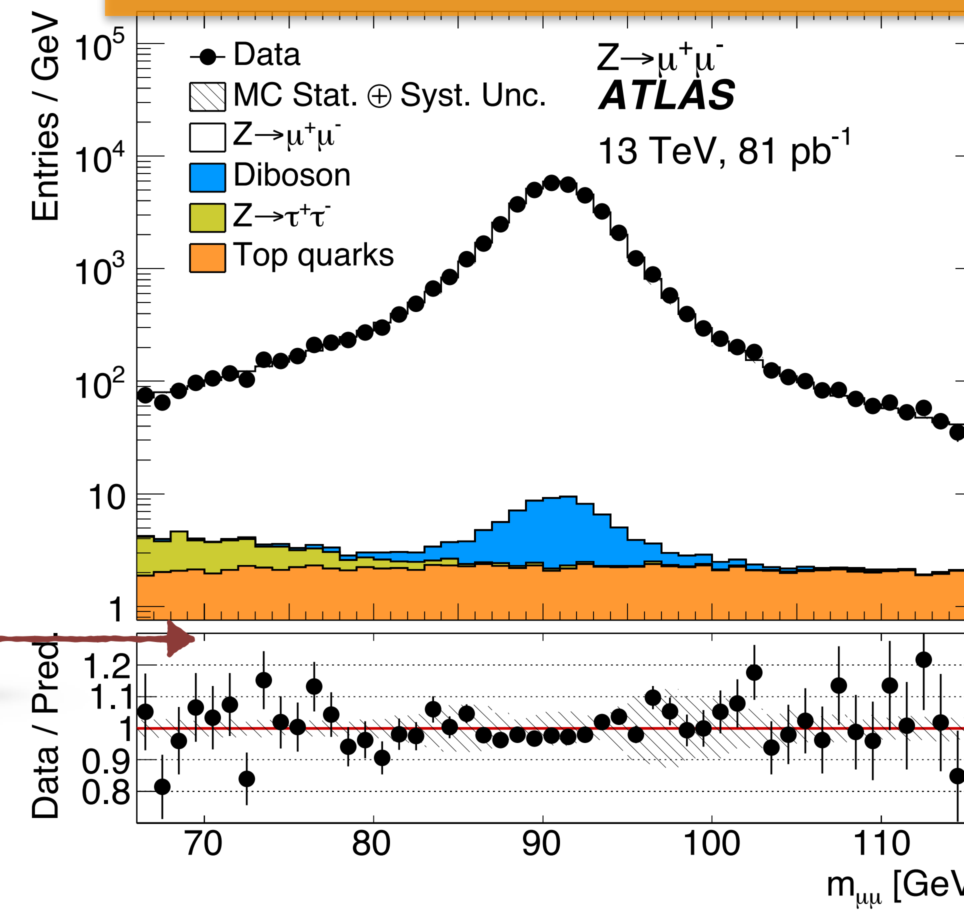

Cross Section strategy:

signal events

$$\sigma^{fid}_{W/Z} \cdot BR(\%) = \frac{N^{obs}_{W/Z} - B_{W/Z}}{C_{W/Z}\, L}$$

Identification, Reconstruction and Trigger Efficiency

Luminosity

Backgrounds:

→ Top-quark and EW from MC (8% for W, 0.7% for Z)

→ **QCD multijet: data driven** (W → eν: 9%, W → μν: 4%)

From fiducial volume to full phase space: $\sigma^{tot}_{W/Z} = \sigma^{fid}_{W/Z} \;/\; A_{W/Z}$

Acceptance (from MCs)

tt/Z cross section ratios 7,8 and 13 TeV

JHEP 02 (2017) 117

Dependence of σ on √s

Single ratio $R_{tt/Z}$ at √s = 13 TeV

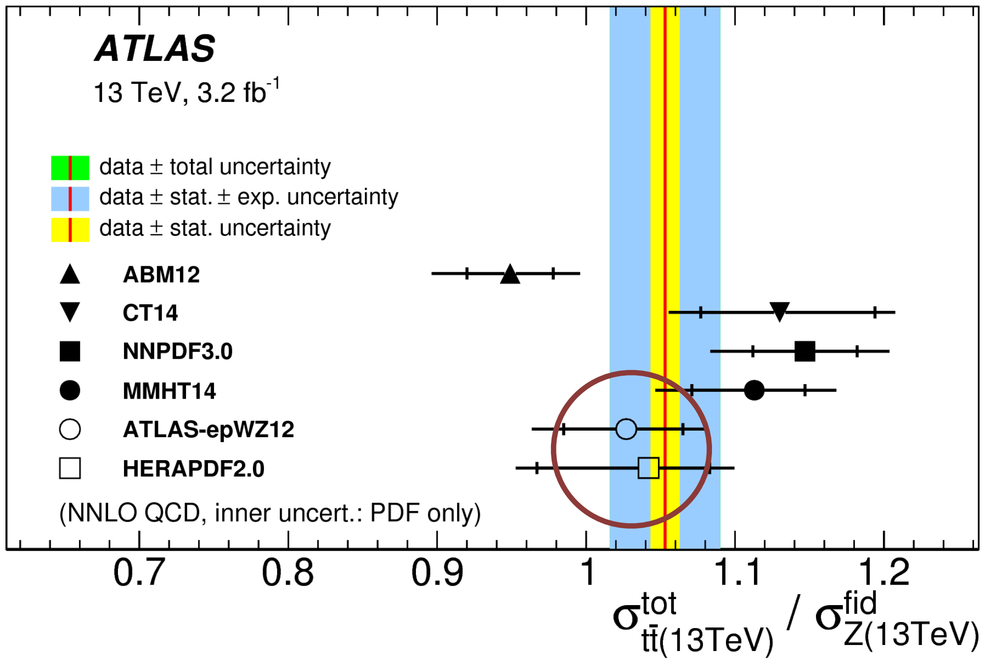

Single ratio $R_{Z(13\ TeV)/Z(8\ TeV)}$

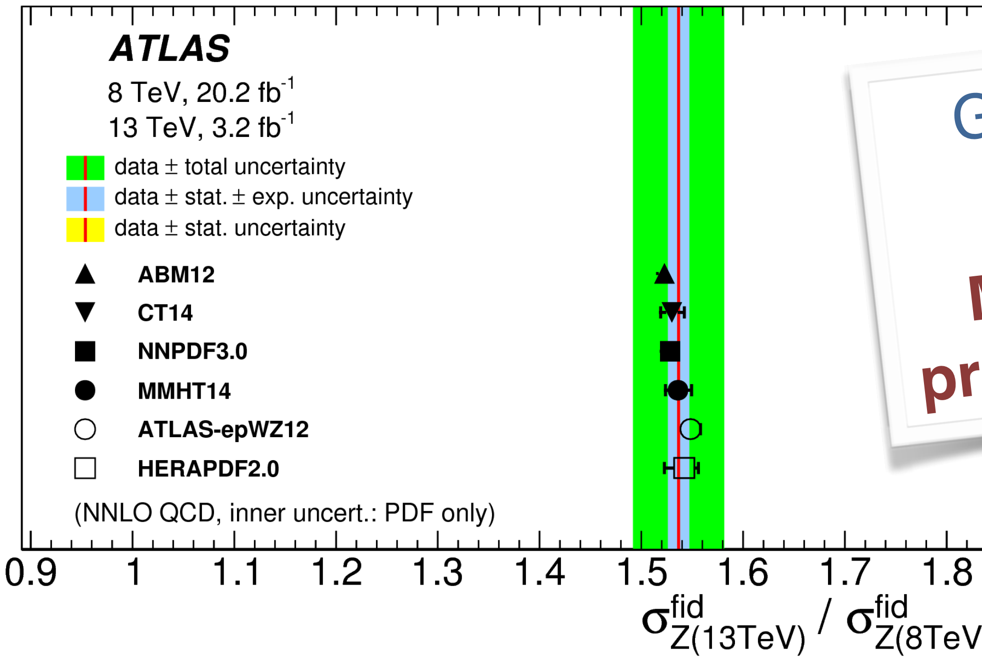

Good agreement with different PDFs

Measurements more precise than predictions

Light quark sea distributions

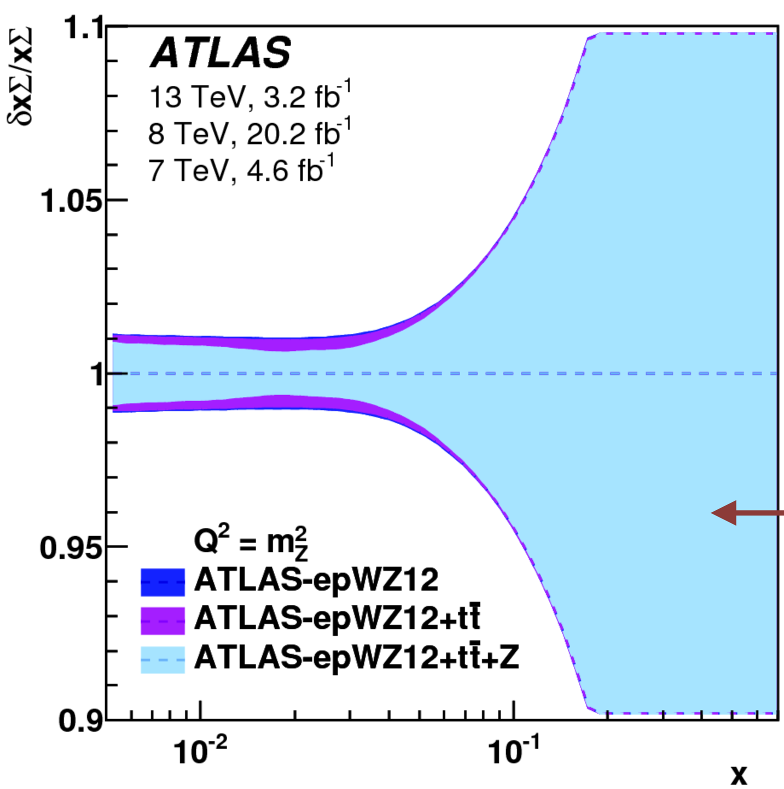

Impact of ATLAS data on the PDF uncertainties quantified by PDF profiling using ATLAS-epWZ12

tt and Z data constraint:

Light quark sea at x < 0.02

Gluon at x ~ 0.1

Gluon distributions

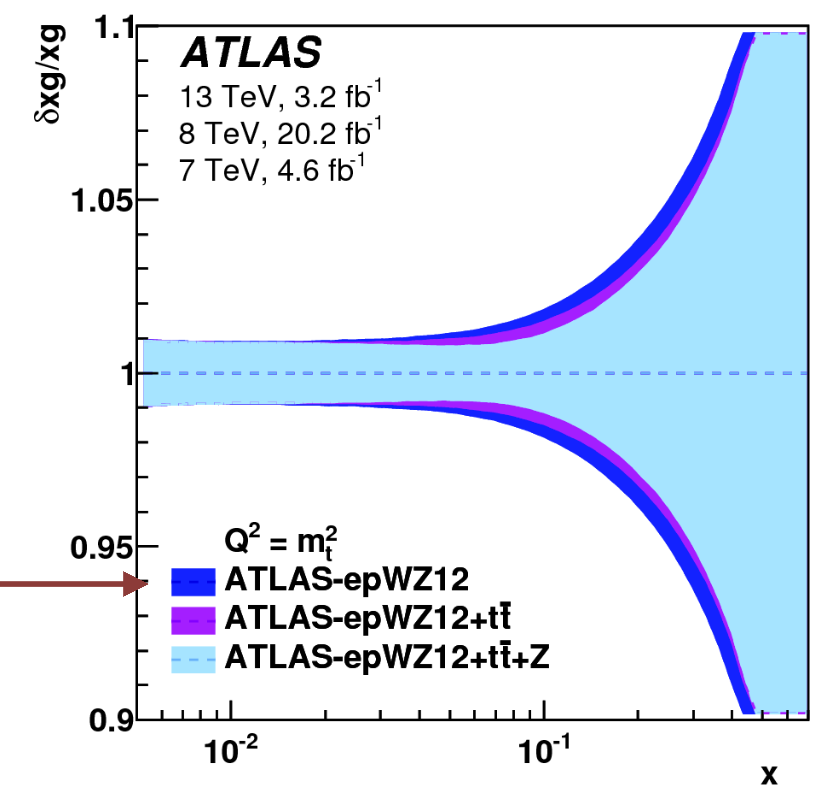

- Higher precision of data comparing to NNLO predictions → constraining power
- Production cross sections more understood @ 7TeV than 13 TeV!
- W^+/W^- well reproduced, for $W^\pm/Z$ all PDFs are systematically higher than data.

Plenty of room for improvement @13 TeV

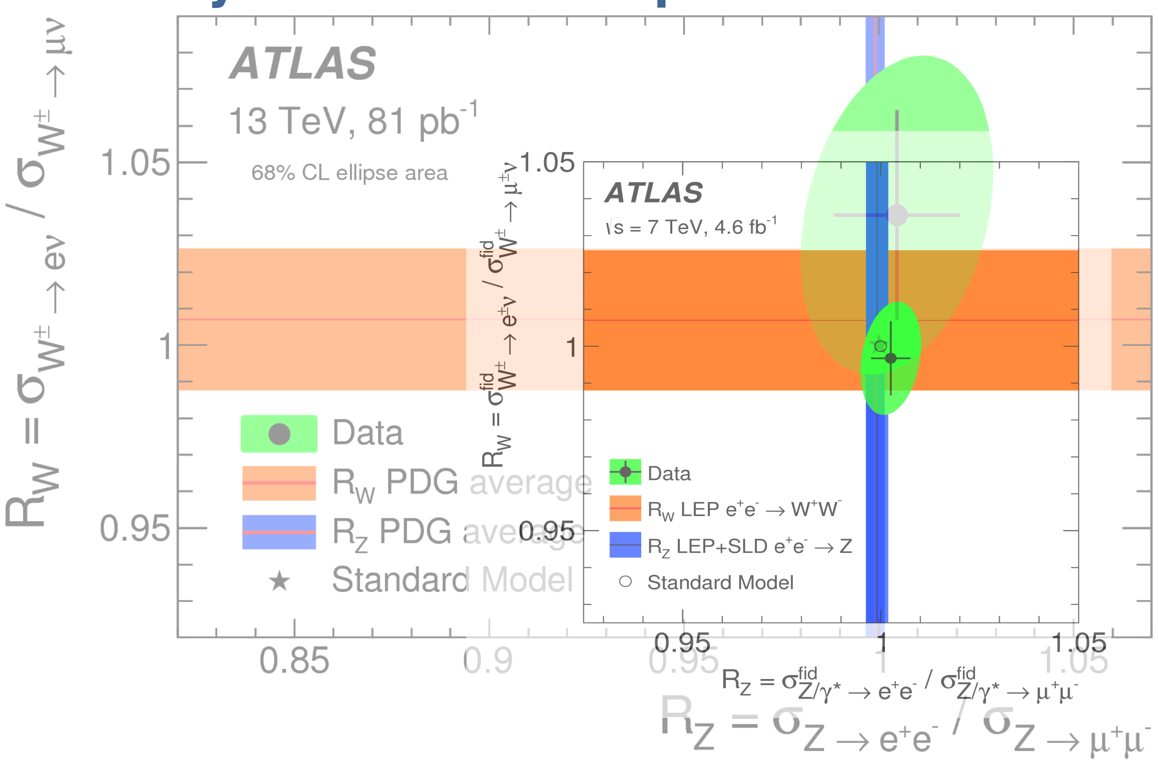

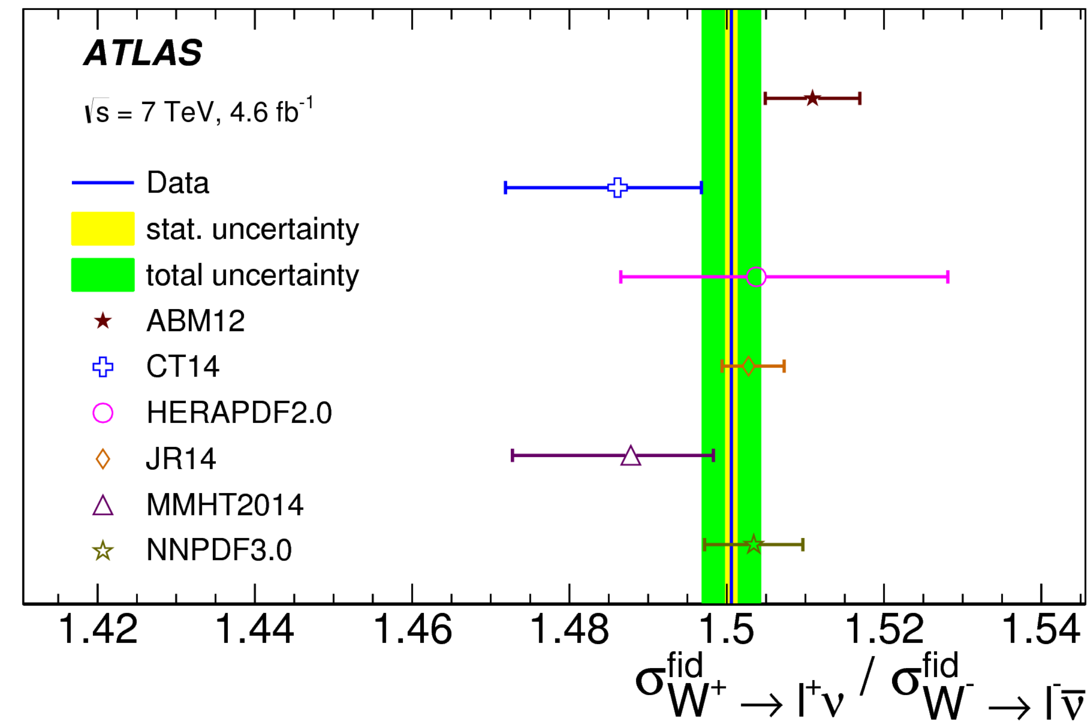

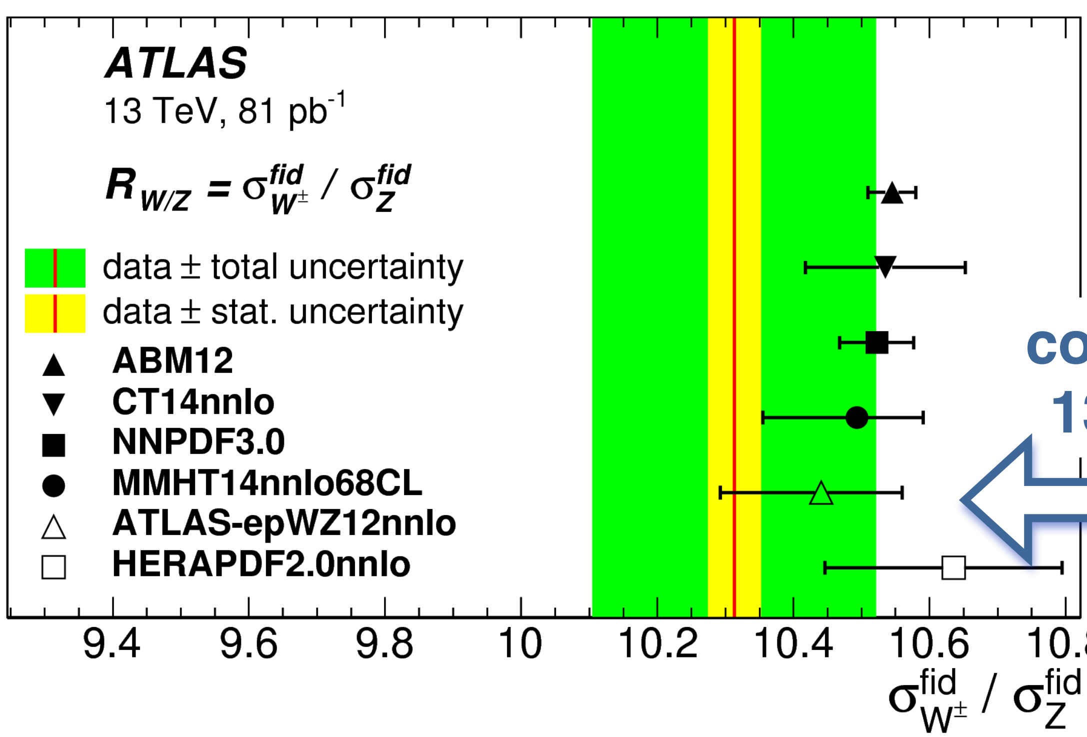

compatible with 13 TeV results

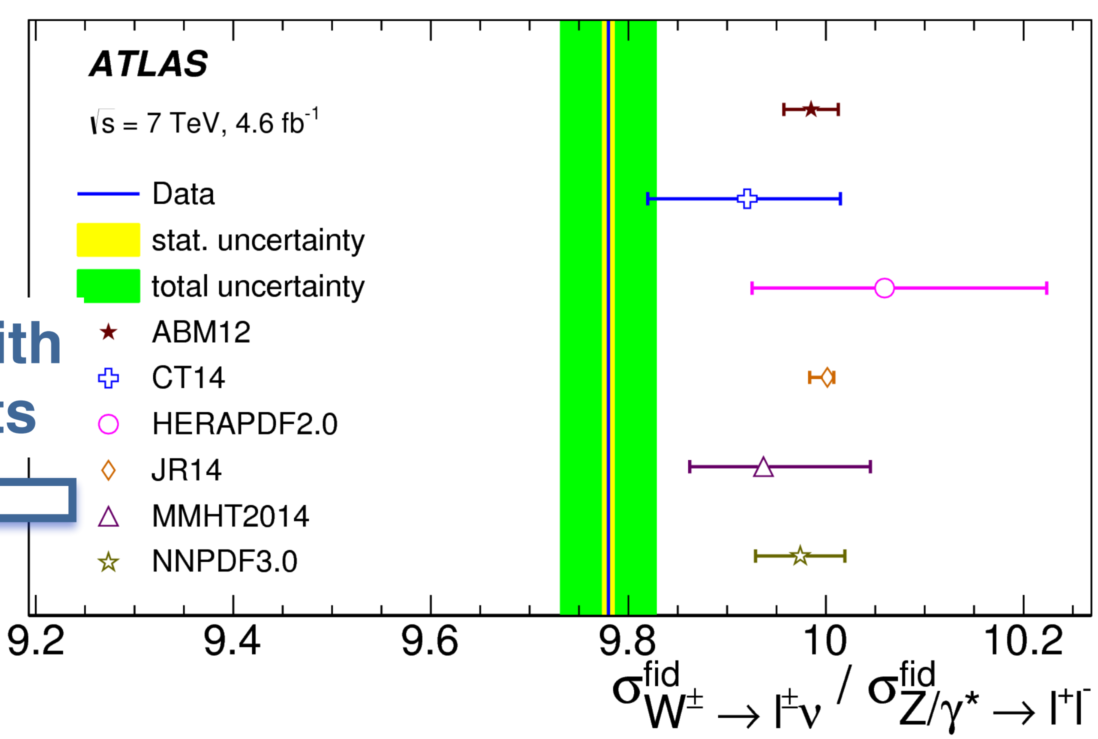

arXiv:1701.07240

✤ **Template fit approach:** compute the p_T^l and m_T distributions for different assumed values of m_W → χ^2 minimisation gives the best fit template

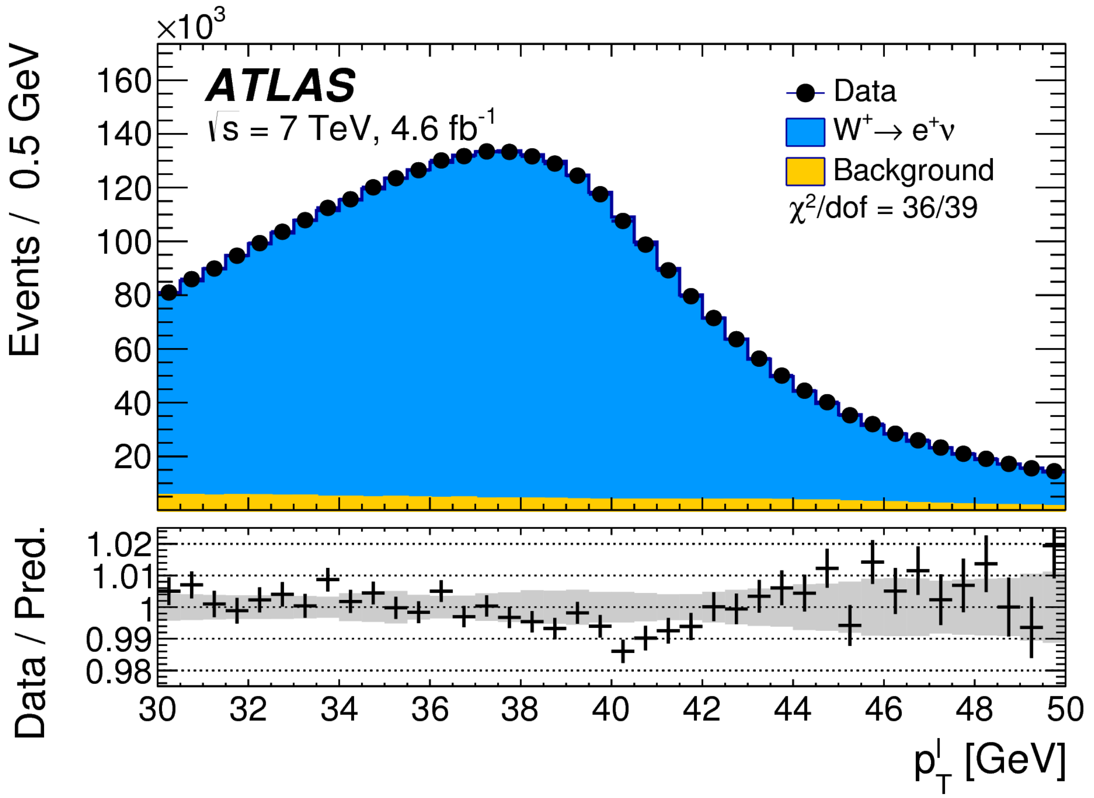

p_T^l has a Jacobian edge at $m_W/2$

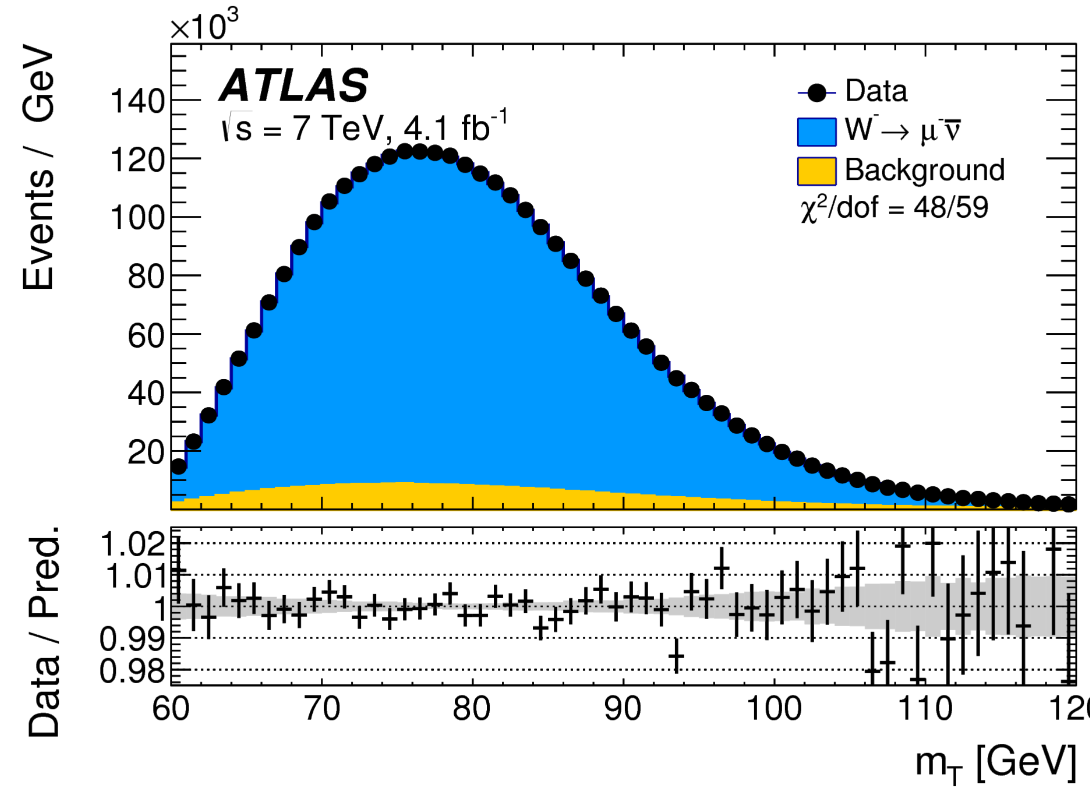

m_T has a Jacobian edge at m_W

W mass · Muon Calibration

- Combined muons from ID+MS tracks
- p_T measurement only from ID → simpler calibration, small loss in resolution
- parametrisation of momentum corrections:

Radial bias (scale)

Resolution correction

$$p_T^{corr} = p_T^{MC} \times \frac{1 + \alpha(\eta,\phi)}{1 + q\,\delta(\eta,\phi)\cdot p_T^{MC}}\left[1 + \beta_{curv}(\eta)\cdot G(0,1)\cdot p_T^{MC}\right]$$

Sagitta bias

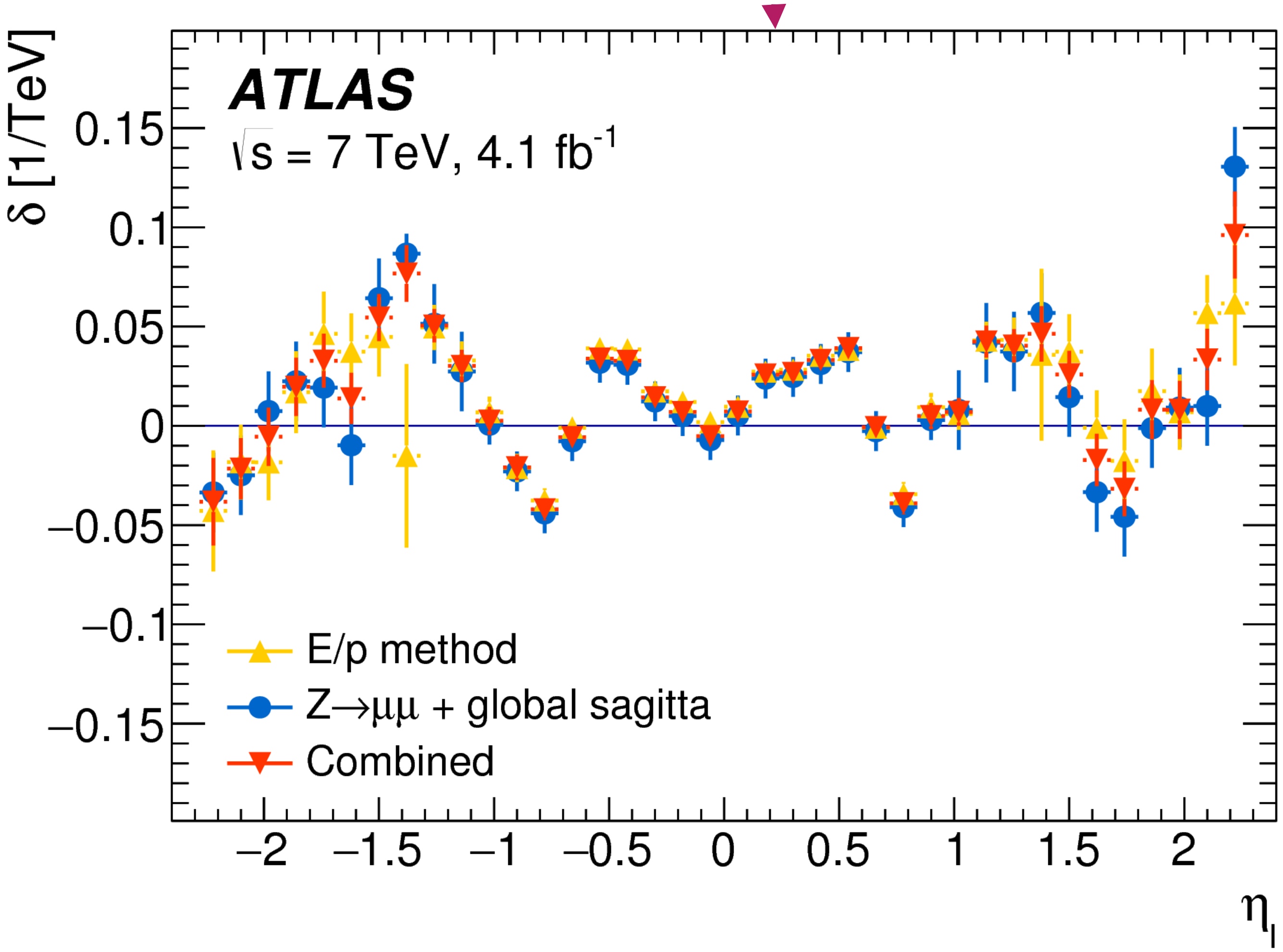

- Charge dependent corrections
- Scale calibrated with 10^{-4} relative unc.
- Scale and resolution corrections derived from Z→μμ line shape
  - ◁Dominant uncertainty derived from the extrapolation Z→W

arXiv:1701.07240

- Calibration of ID muons using Z

$$k^c = (\boxed{A} - 1)k + \boxed{qM} + \boxed{\frac{k}{1 + k\,\epsilon \sin\theta}}$$

magnetic field

mis-alignement

material

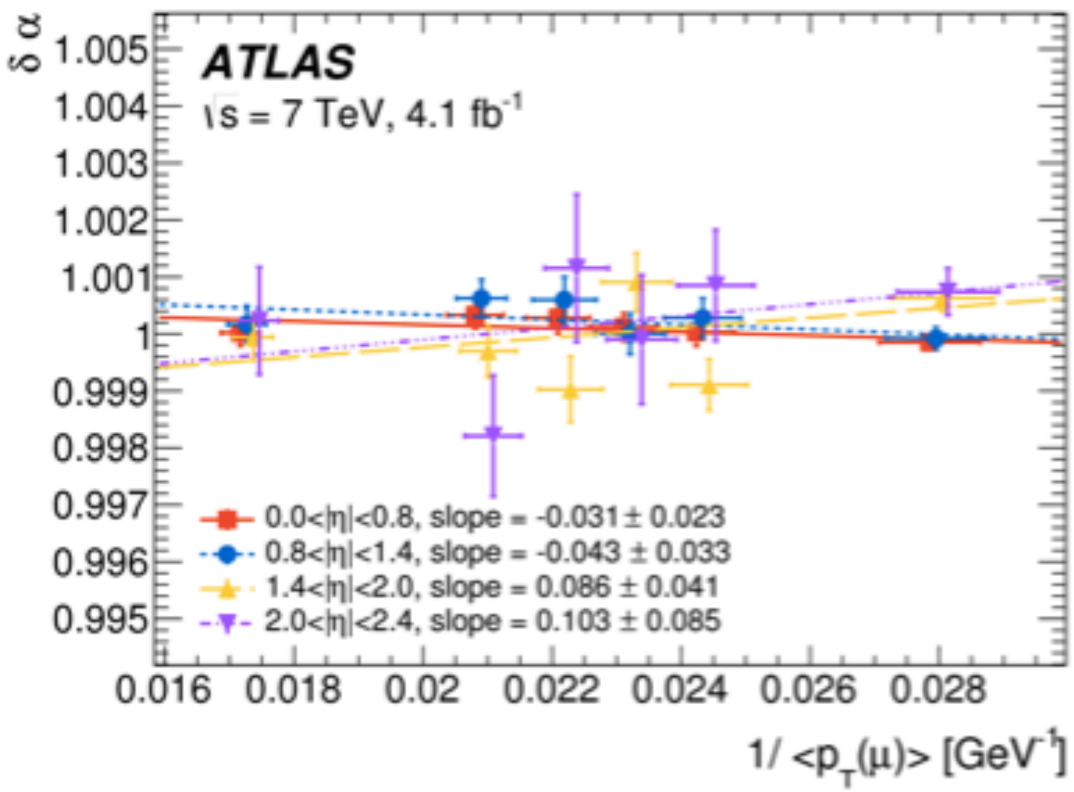

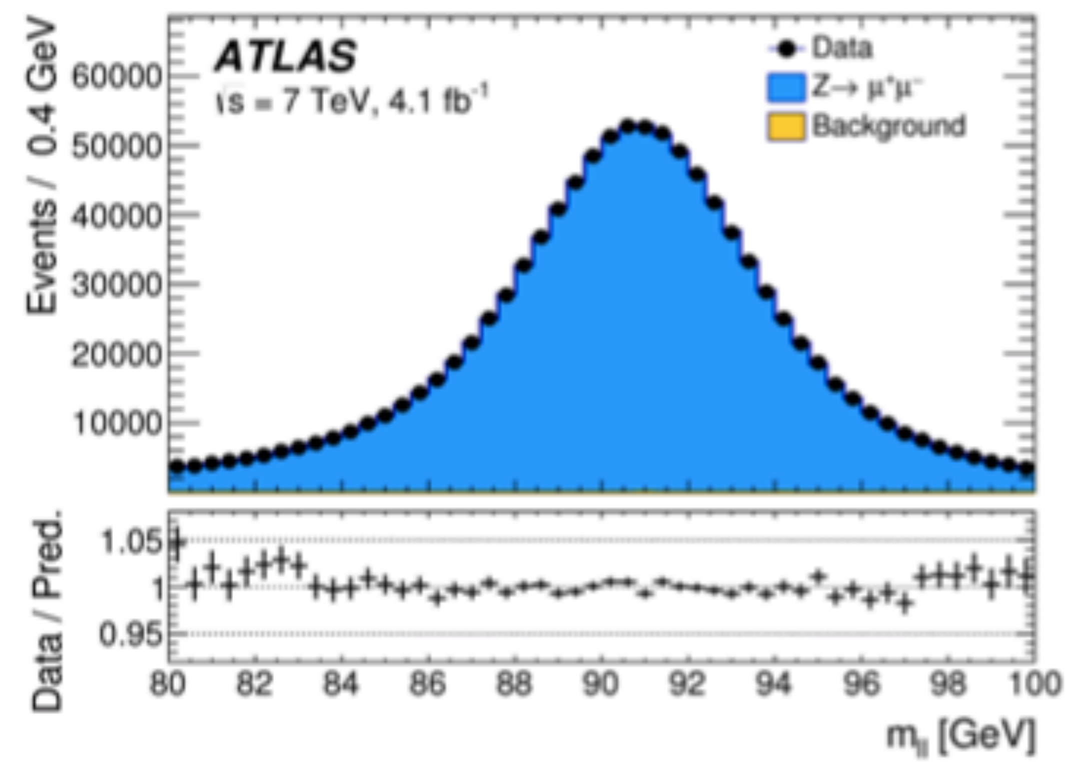

$\lvert\eta_\ell\rvert$ range	[0.0, 0.8]		[0.8, 1.4]		[1.4, 2.0]		[2.0, 2.4]		Combined	
Kinematic distribution	p_T^ℓ	m_T	p_T^ℓ	m_T	p_T^ℓ	m_T	p_T^ℓ	m_T	p_T^ℓ	m_T
δm_W [MeV]										
Momentum scale	8.9	9.3	14.2	15.6	27.4	29.2	111.0	115.4	8.4	8.8
Momentum resolution	1.8	2.0	1.9	1.7	1.5	2.2	3.4	3.8	1.0	1.2
Sagitta bias	0.7	0.8	1.7	1.7	3.1	3.1	4.5	4.3	0.6	0.6
Reconstruction and isolation efficiencies	4.0	3.6	5.1	3.7	4.7	3.5	6.4	5.5	2.7	2.2
Trigger efficiency	5.6	5.0	7.1	5.0	11.8	9.1	12.1	9.9	4.1	3.2
Total	11.4	11.4	16.9	17.0	30.4	31.0	112.0	116.1	9.8	9.7

arXiv:1701.07240

✤ Exclude bin 1.2<|eta|<1.82 as the amount of passive material and its uncertainty are largest

Eur.Phys.J.C 74 (2014) 3071

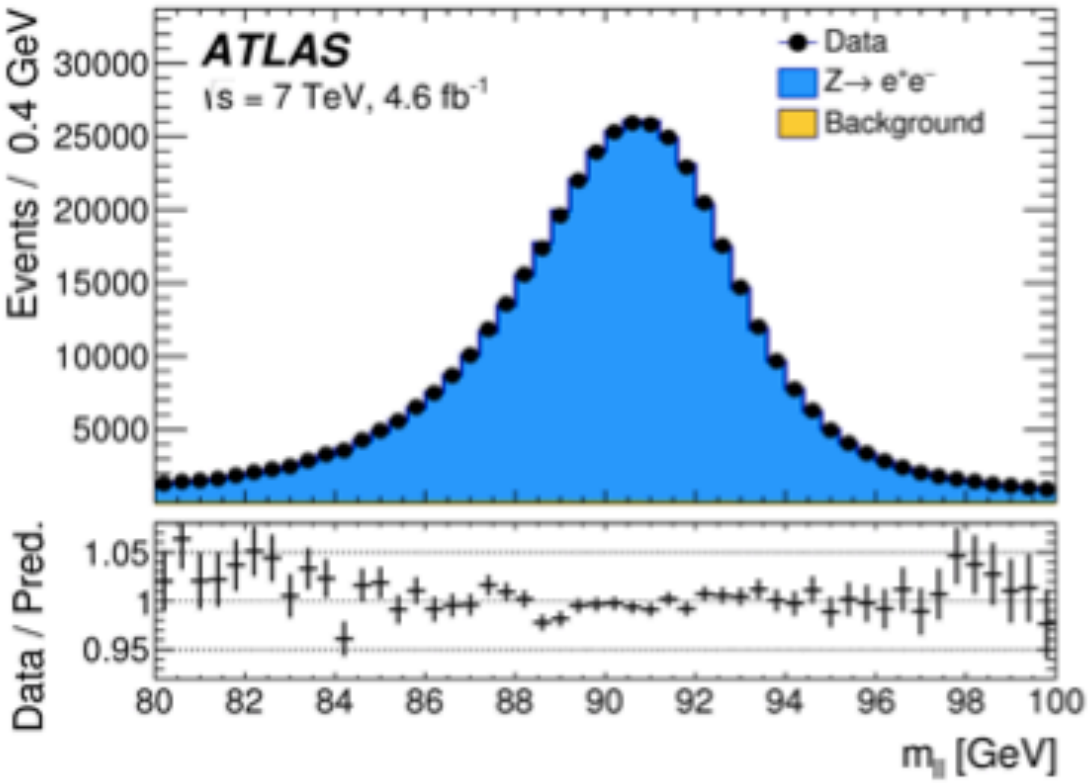

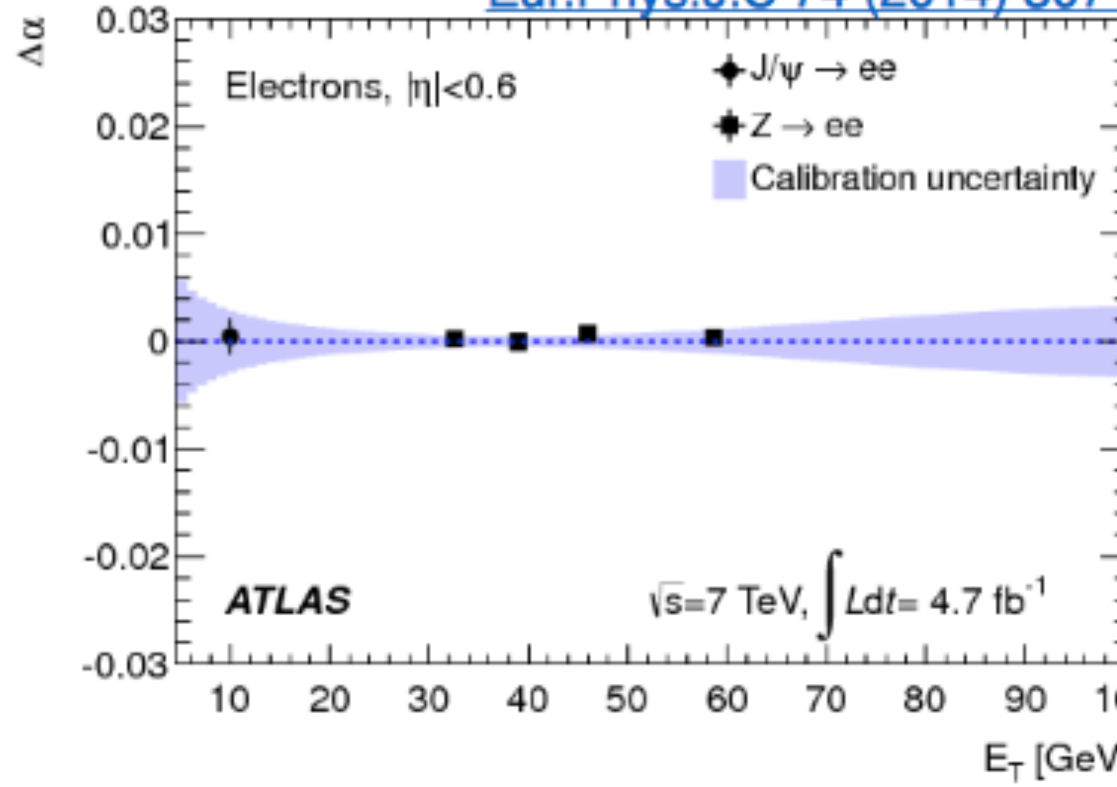

$\lvert\eta_\ell\rvert$ range	[0.0, 0.6]		[0.6, 1.2]		[1.82, 2.4]		Combined	
Kinematic distribution	p_T^ℓ	m_T	p_T^ℓ	m_T	p_T^ℓ	m_T	p_T^ℓ	m_T
δm_W [MeV]								
Energy scale	10.4	10.3	10.8	10.1	16.1	17.1	8.1	8.0
Energy resolution	5.0	6.0	7.3	6.7	10.4	15.5	3.5	5.5
Energy linearity	2.2	4.2	5.8	8.9	8.6	10.6	3.4	5.5
Energy tails	2.3	3.3	2.3	3.3	2.3	3.3	2.3	3.3
Reconstruction efficiency	10.5	8.8	9.9	7.8	14.5	11.0	7.2	6.0
Identification efficiency	10.4	7.7	11.7	8.8	16.7	12.1	7.3	5.6
Trigger and isolation efficiencies	0.2	0.5	0.3	0.5	2.0	2.2	0.8	0.9
Charge mismeasurement	0.2	0.2	0.2	0.2	1.5	1.5	0.1	0.1
Total	19.0	17.5	21.1	19.4	30.7	30.5	14.2	14.3

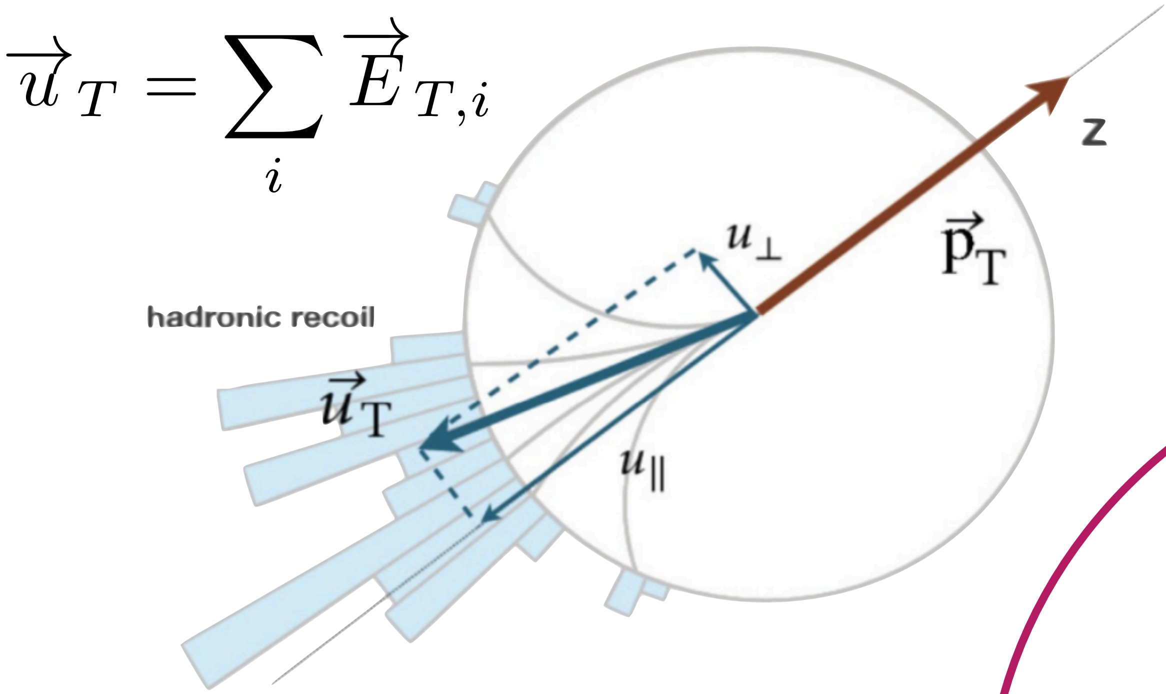

- Recoil u_T is a measure of p_T^W
- Calibration steps:
  - ◁ correct pile-up in MC to match data
  - ◁ correct for residual differences in the $\sum E_T$ distribution
  - ◁ derive scale and resolution corrections from p_T balance in Z events

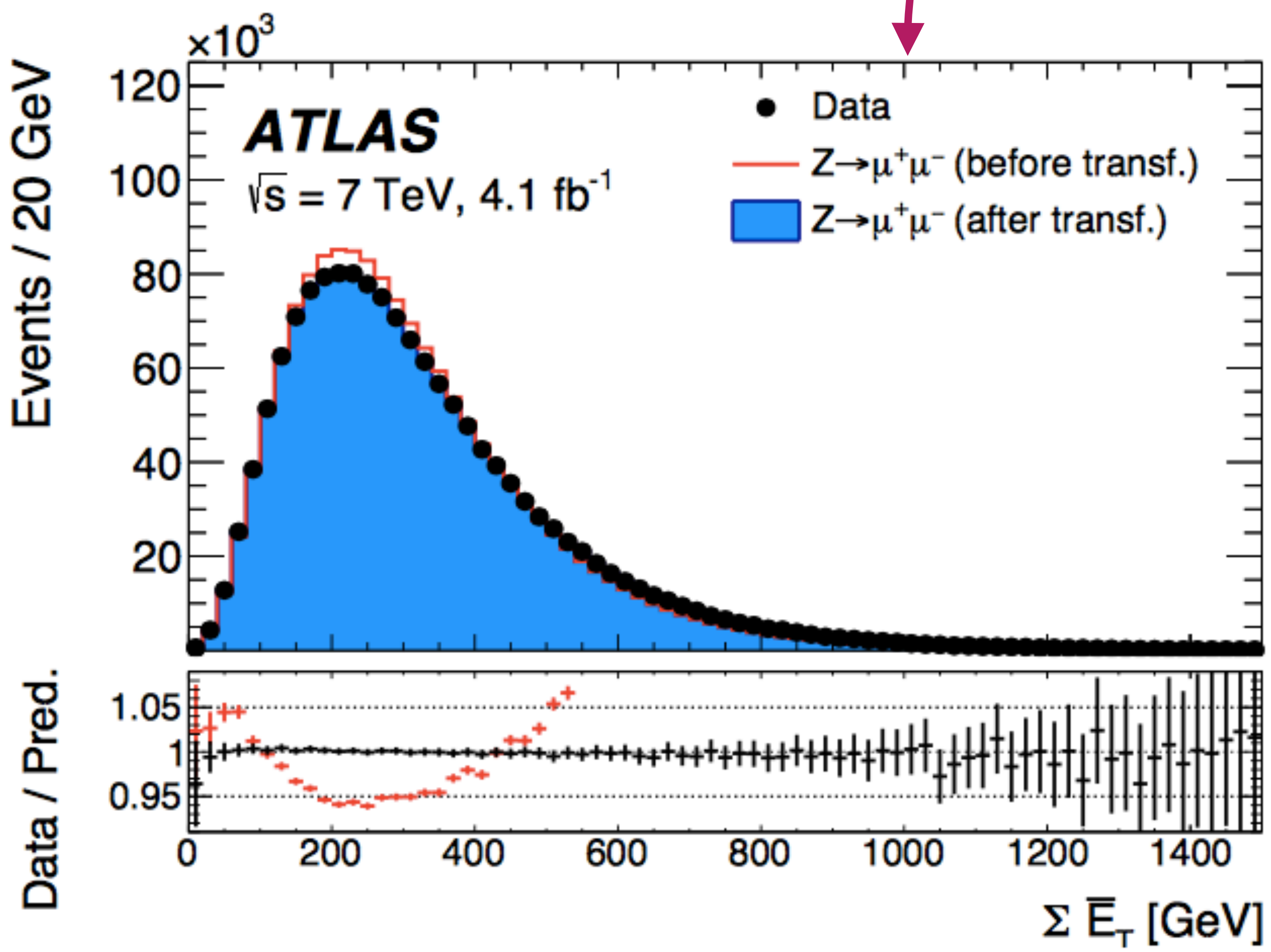

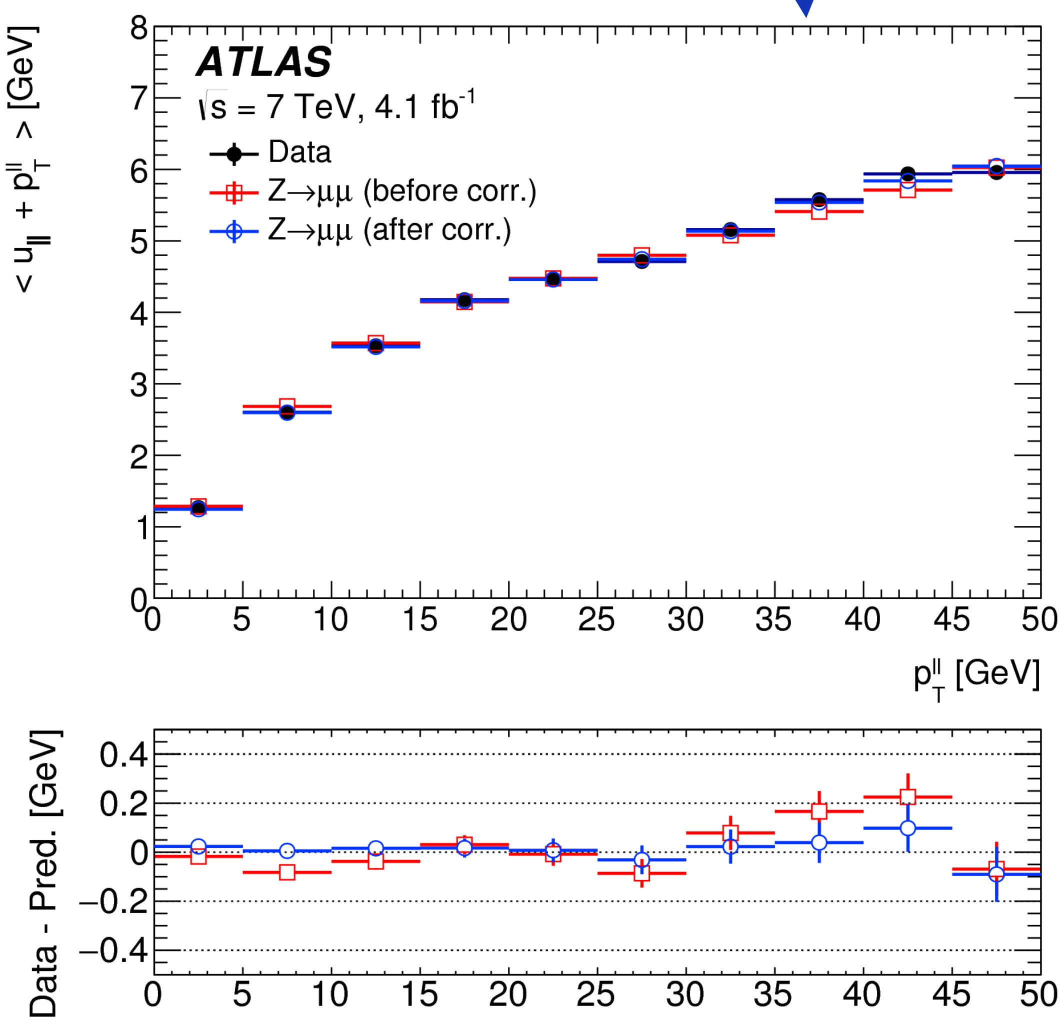

arXiv:1701.07240

- Vector sum of the moment of all clusters measured in the calorimeters
- Calibrate the scale (resolution) of the recoil using ull (u⊥) from Z events

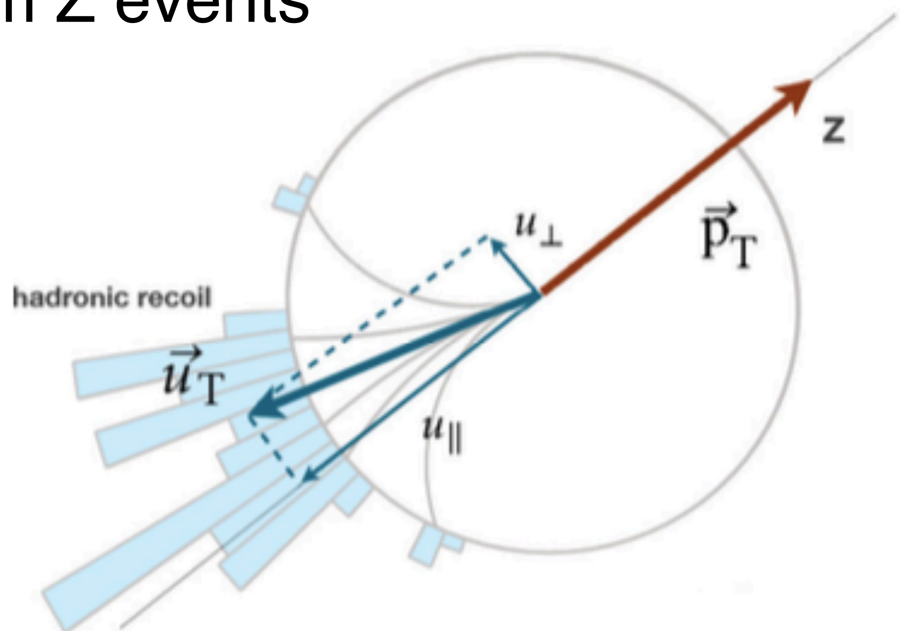

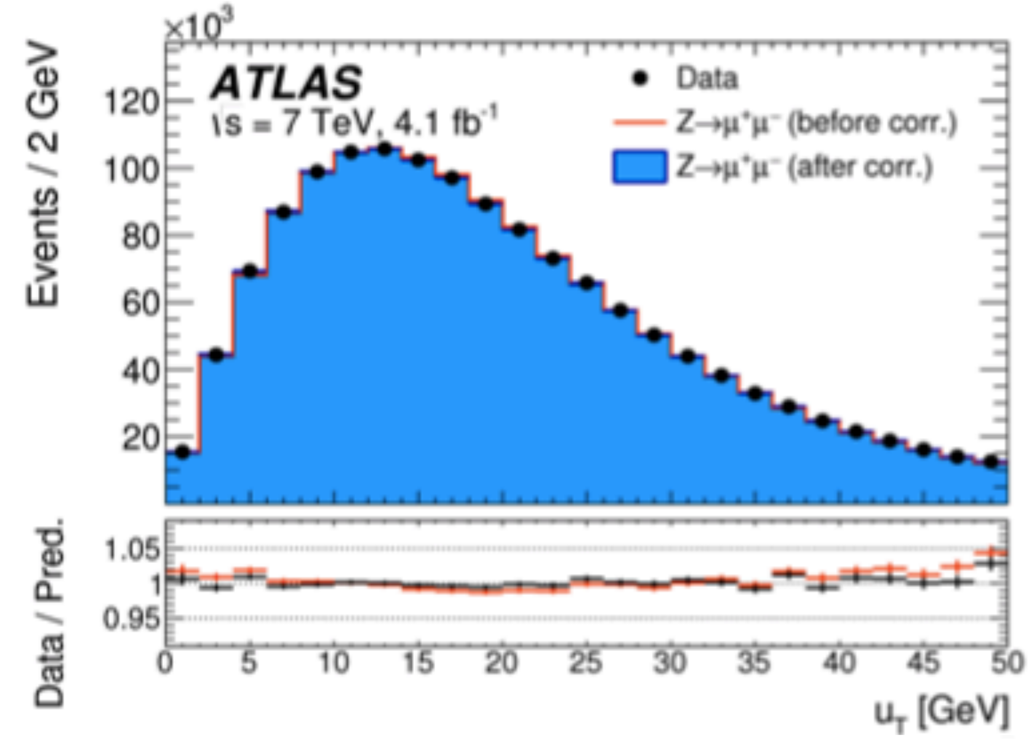

ATLAS

W-boson charge	W^+		W^-		Combined	
Kinematic distribution	p_T^ℓ	m_T	p_T^ℓ	m_T	p_T^ℓ	m_T
δm_W [MeV]						
$\langle\mu\rangle$ scale factor	0.2	1.0	0.2	1.0	0.2	1.0
$\Sigma\bar{E}_T$ correction	0.9	12.2	1.1	10.2	1.0	11.2
Residual corrections (statistics)	2.0	2.7	2.0	2.7	2.0	2.7
Residual corrections (interpolation)	1.4	3.1	1.4	3.1	1.4	3.1
Residual corrections ($Z \to W$ extrapolation)	0.2	5.8	0.2	4.3	0.2	5.1
Total	2.6	14.2	2.7	11.8	2.6	13.0

W mass · Compatibility of categories

- Same strategy performed in 28 different categories in p_T^W and m_T^W

Decay channel	$W \to e\nu$	$W \to \mu\nu$
Kinematic distributions	p_T^ℓ, m_T	p_T^ℓ, m_T
Charge categories	W^+, W^-	W^+, W^-
$\lvert\eta_\ell\rvert$ categories	$[0, 0.6]$, $[0.6, 1.2]$, $[1.8, 2.4]$	$[0, 0.8]$, $[0.8, 1.4]$, $[1.4, 2.0]$, $[2.0, 2.4]$